Some Applications of Coherent X-rays from a 3rd Generation Synchrotron Source

Tetsuya Ishikawa

RIKEN Harima Institute

8/5/2010 KITP, UCSB, Santa Barbara, CA, USA

Collaborators

RIKEN

Kenji Tamasaku, Yoshihito Tanaka, Yoshiki Kohmura, Kei Sawada, Hideo Kitamura, Masaki Yamamoto, Tsumoru Shintake, Cyonyang Song, Alfred Baron, Masaki Takata, Noritaka Kumagai, Hiroaki Maeshima

JASRI

Makina Yabashi, Hiroshi Yamazaki, Haruhiko Ohashi, Shunji Goto

Osaka University

Kazuto Yamauchi, Yukio Takahashi

Hokkaido University

Yoshinori Nishino

UCLA

John Miao

Plan

- Introduction
- Coherence Measurement
  - X-Ray HBT interferometer
  - X-Ray Michelson Interferometer & X-ray FT spectroscopy
- Non Linear X-Ray Optics
  - Parametric Down Conversion
- X-Ray Mirror Development using 1000 m BL
  - Flat Mirror
  - KB Focusing
  - Sub 10 nm Focusing
- Present Status of Japan X-Ray Free Electron Laser Project
- Summary

New Lights Always Create New Science & Technology

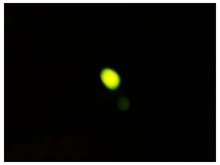

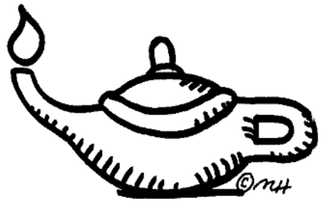

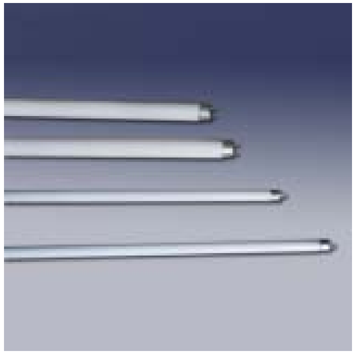

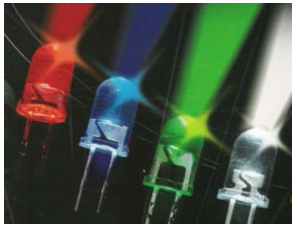

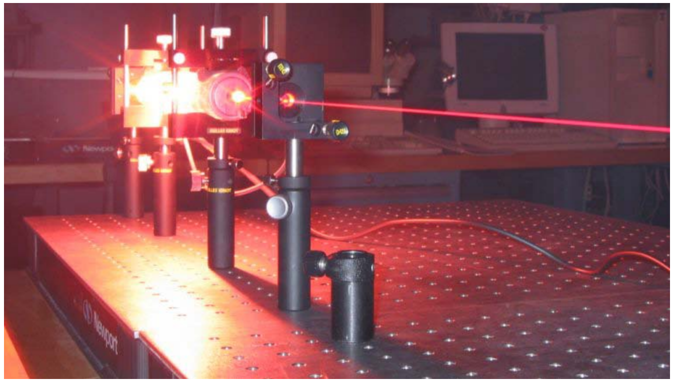

Coherence: One of the most significant feature of 3rd generation SR sources

Applications of Coherent X-Rays: 2004 Jpn SR Society Meeting

- Coherent Diffraction
- Holography
- Photon Correlation Spectroscopy
- Propagation-based Imaging
- Nano-beam Micrography
- Non-Linear Optics

What astonished us at that time…

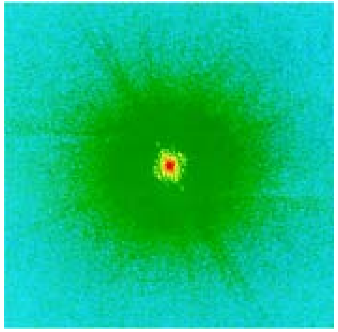

CDI of E-Coli
*J. Miao et al: PNAS, **100**, 110 (2003).*

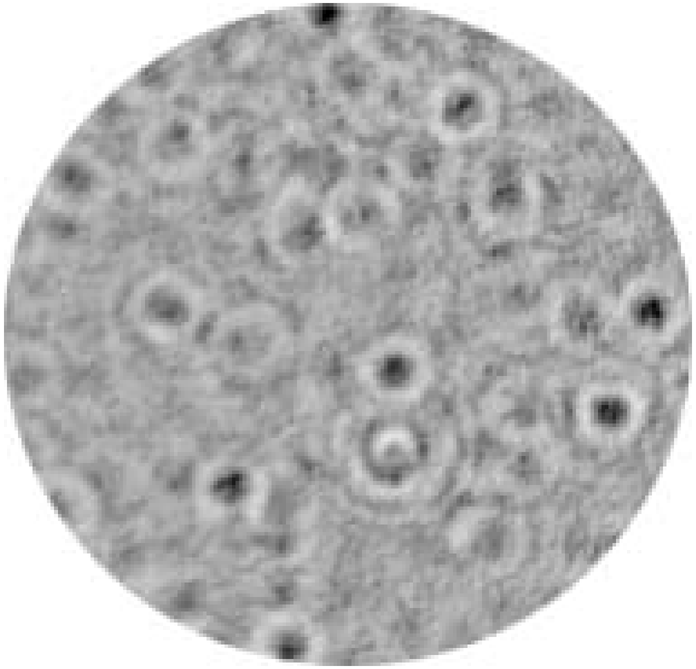

X-Ray Speckles from a Be window

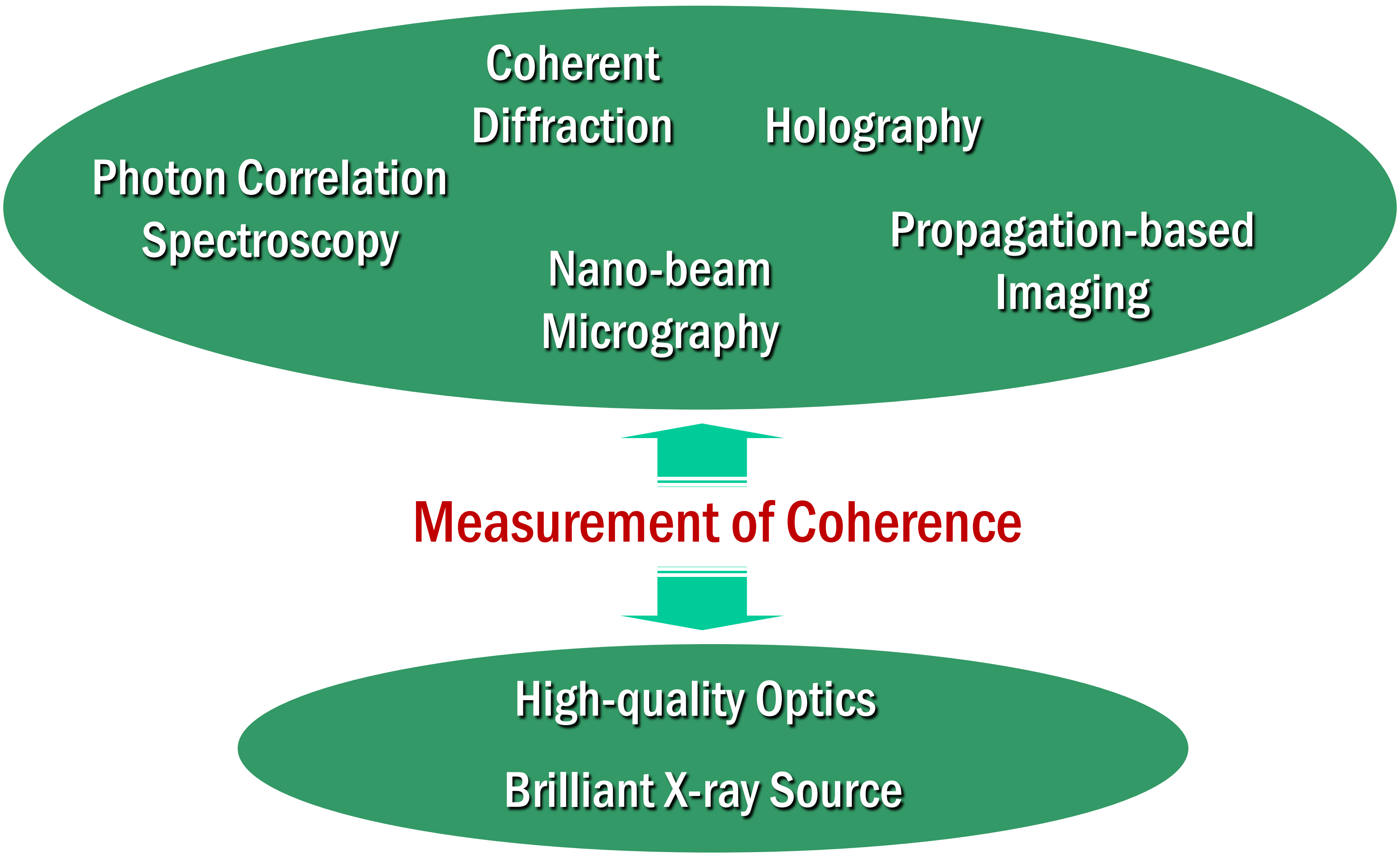

Coherent Diffraction
Holography
Photon Correlation Spectroscopy
Propagation-based Imaging
Nano-beam Micrography
Measurement of Coherence
High-quality Optics
Brilliant X-ray Source

Coherence Measurement Interferometer

Amplitude Interferometer

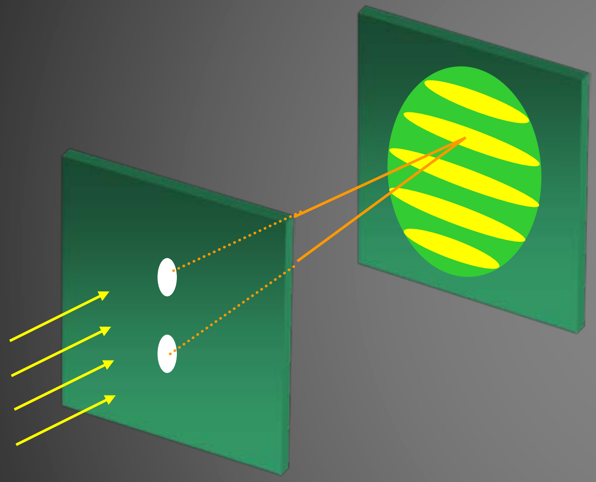

Thomas Young, 1807

Intensity Interferometer

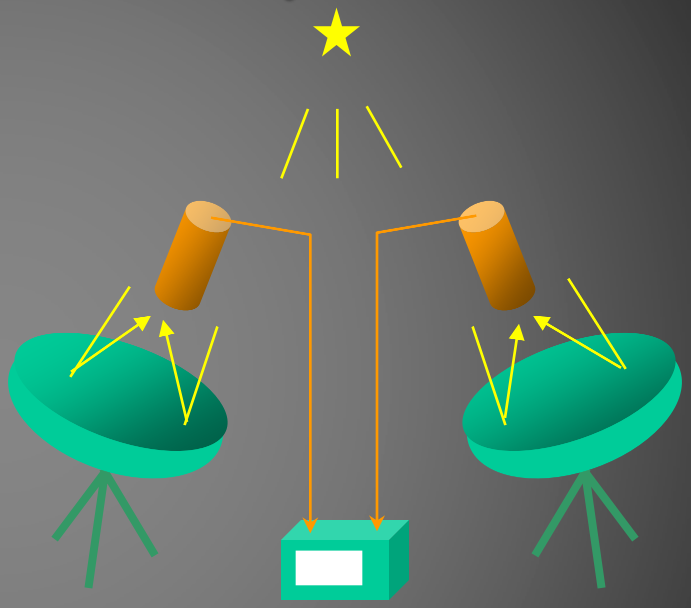

Hanbury-Brown and Twiss, 1956

Intensity Interferometer

Pro	Con
▪ Optics could be unstable	▪ Need High Brilliance Light
▪ Optics could be simple	▪ Need Monochromatization
▪ Photon Statutistic Information	

Short History

1807	Young	Amplitude Interference using Double Slits
1956	HBT	Intensity Interference using Hg lamp(Nature)
1974	Shuryak	Proposal of SR diagonostic application (JETP)
1992	Ikonen	Estimation for 3rd generation SR(PRL)
1997	Kikuta *et al.*	First HX data (E=14.4 keV, R~0.6 %) (JSR)
1999	Miyahara *et al.*	First SX data(E=70 eV, R~1 %) (PRA)
2000	Gluskin *et al.*	HX data from APS (E=14.4 keV, R~1 %) (JSR)

1998 ~ 2000 Coherent X-ray Optics Beamlines at SPring-8
BL29XU and 19LXU

Source

Coherent Source

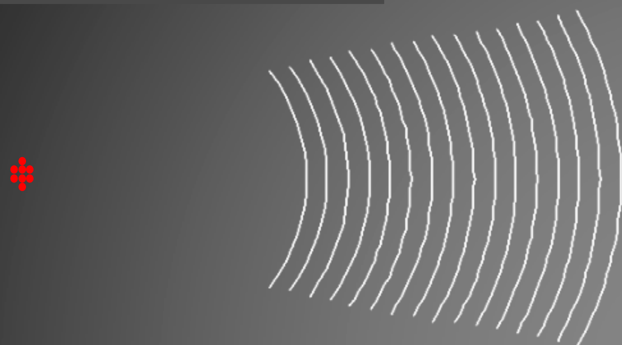

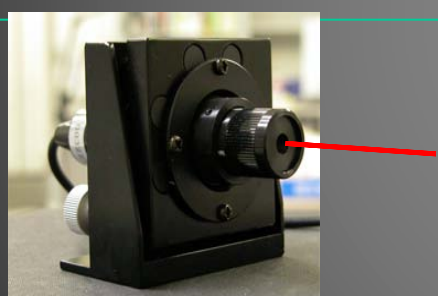

Chaotic Source

Temporal & Spatial Coherence

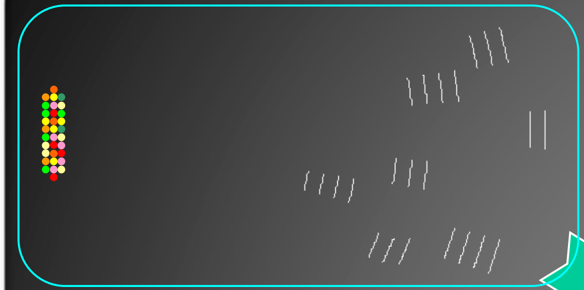

Spatial Coherence Length

Source size, Distance from the source

$$\sigma_y \propto \frac{\lambda L}{s_y}$$

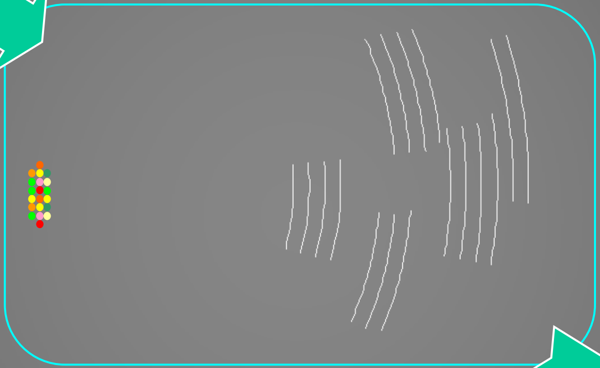

Temporal Coherence Length

Bandpass

$$\sigma_t \propto \frac{1}{\Delta E}$$

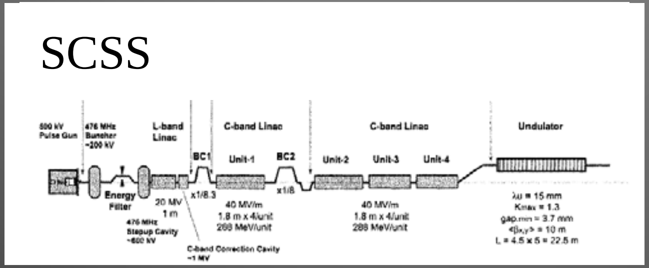

Chaotic field

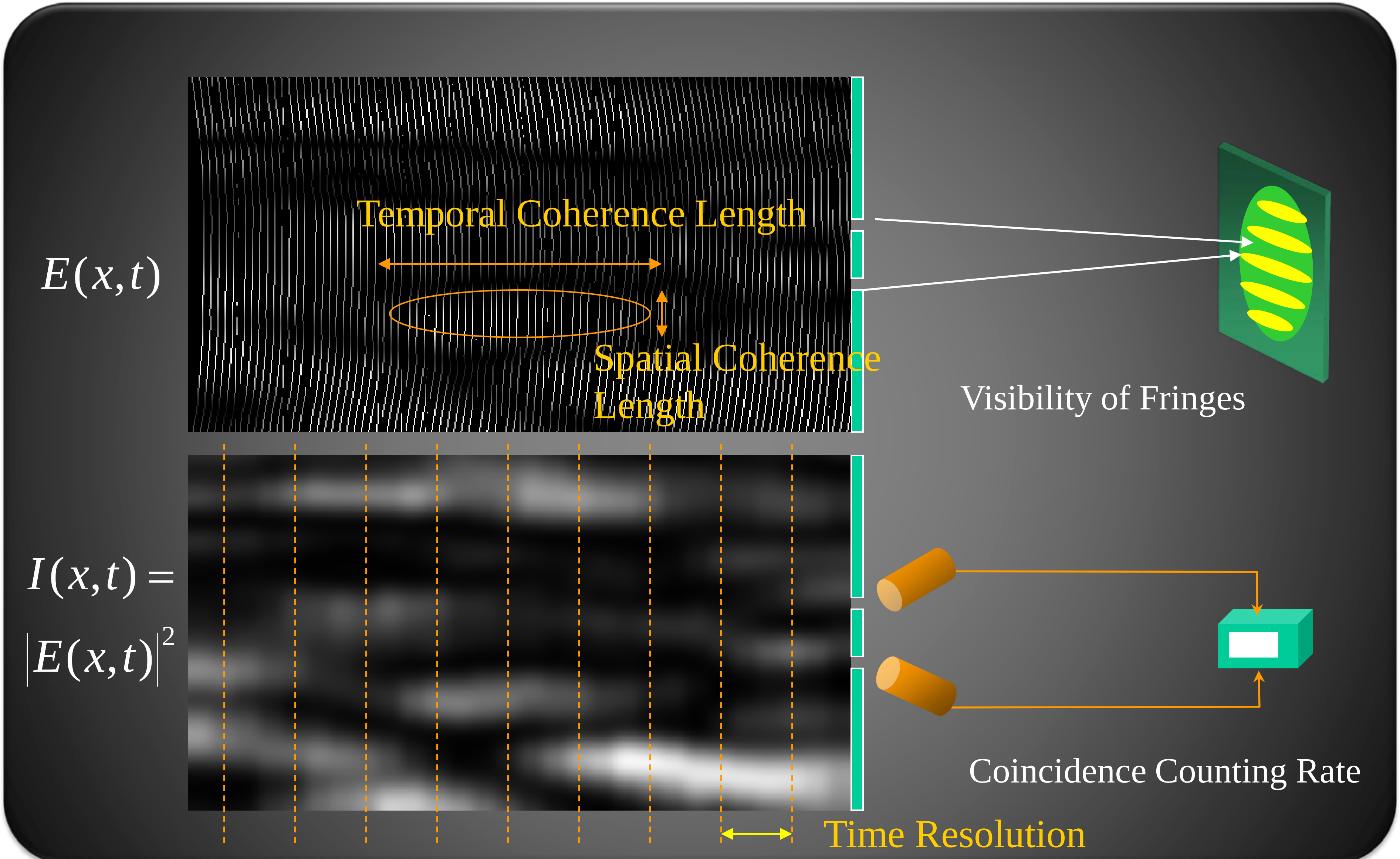

Principle

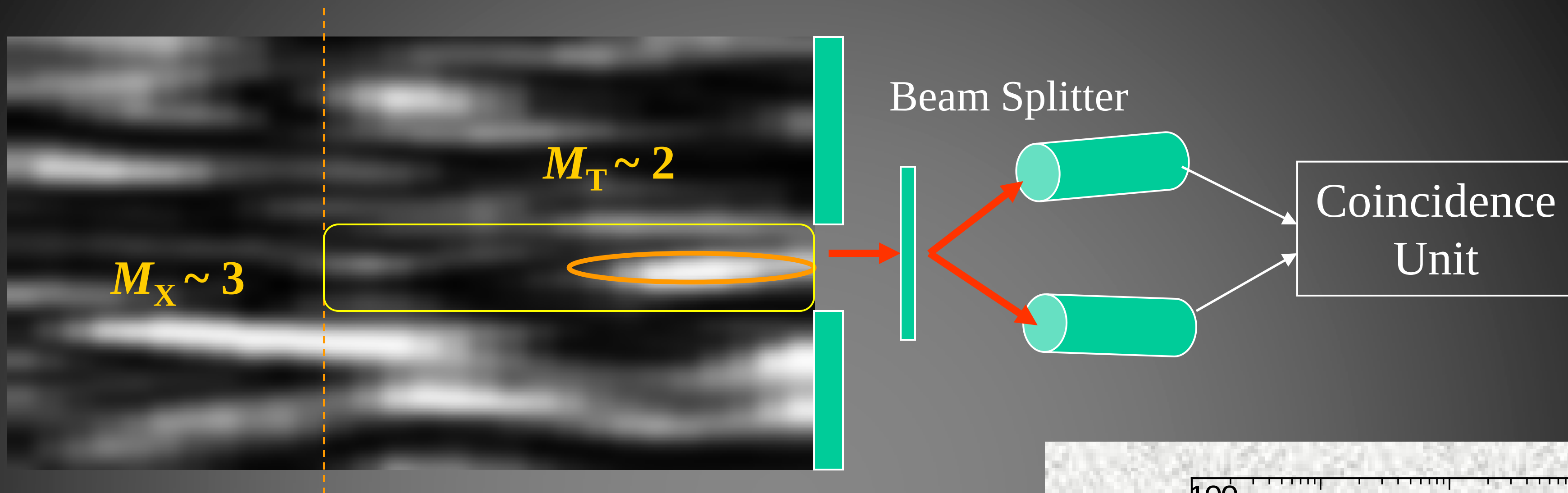

Mode number: $M = M_X M_Y M_T$

Smaller M → Larger Intensity Fluctuation

→ Larger Coincidence Count Rate

$$\langle I_A I_B \rangle = \langle I_A \rangle \langle I_B \rangle (1 + 1/M)$$

$$R \equiv \frac{\langle I_A I_B \rangle}{\langle I_A \rangle \langle I_B \rangle} - 1 = \frac{1}{M}$$

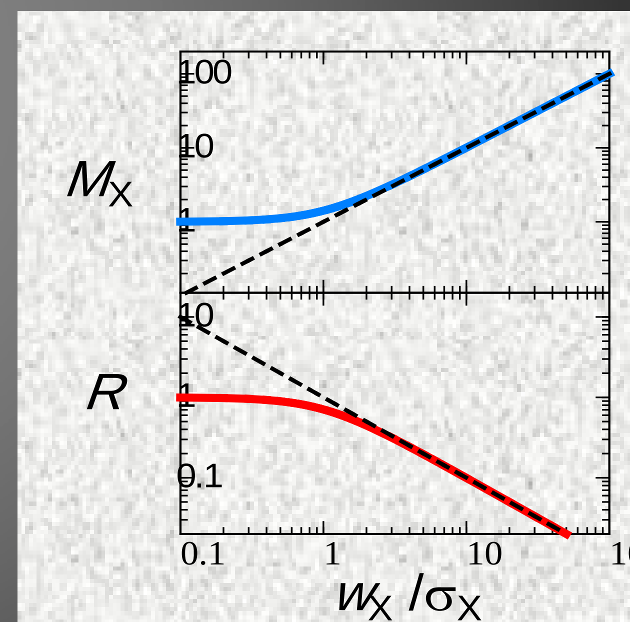

Longitudinal Mode Number

$$M_T = \sqrt{1 + \left(\frac{s_T}{\sigma_T}\right)^2}$$

$$= \sqrt{1 + \left(\frac{s_T \cdot \Delta E}{4h \ln 2}\right)^2}$$

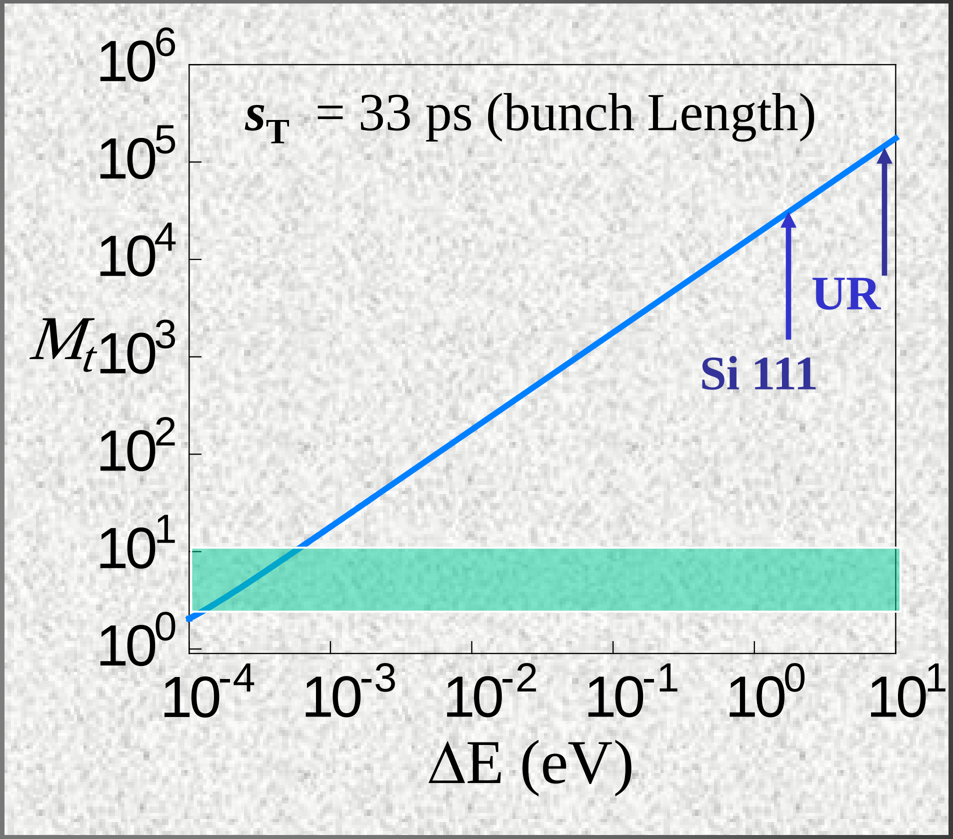

$\mathbf{M_T < 10}$

ΔE ~ ***sub*** **meV**

Need High Resolution Monochromator (HRM)

HRM Development (up to 2000)

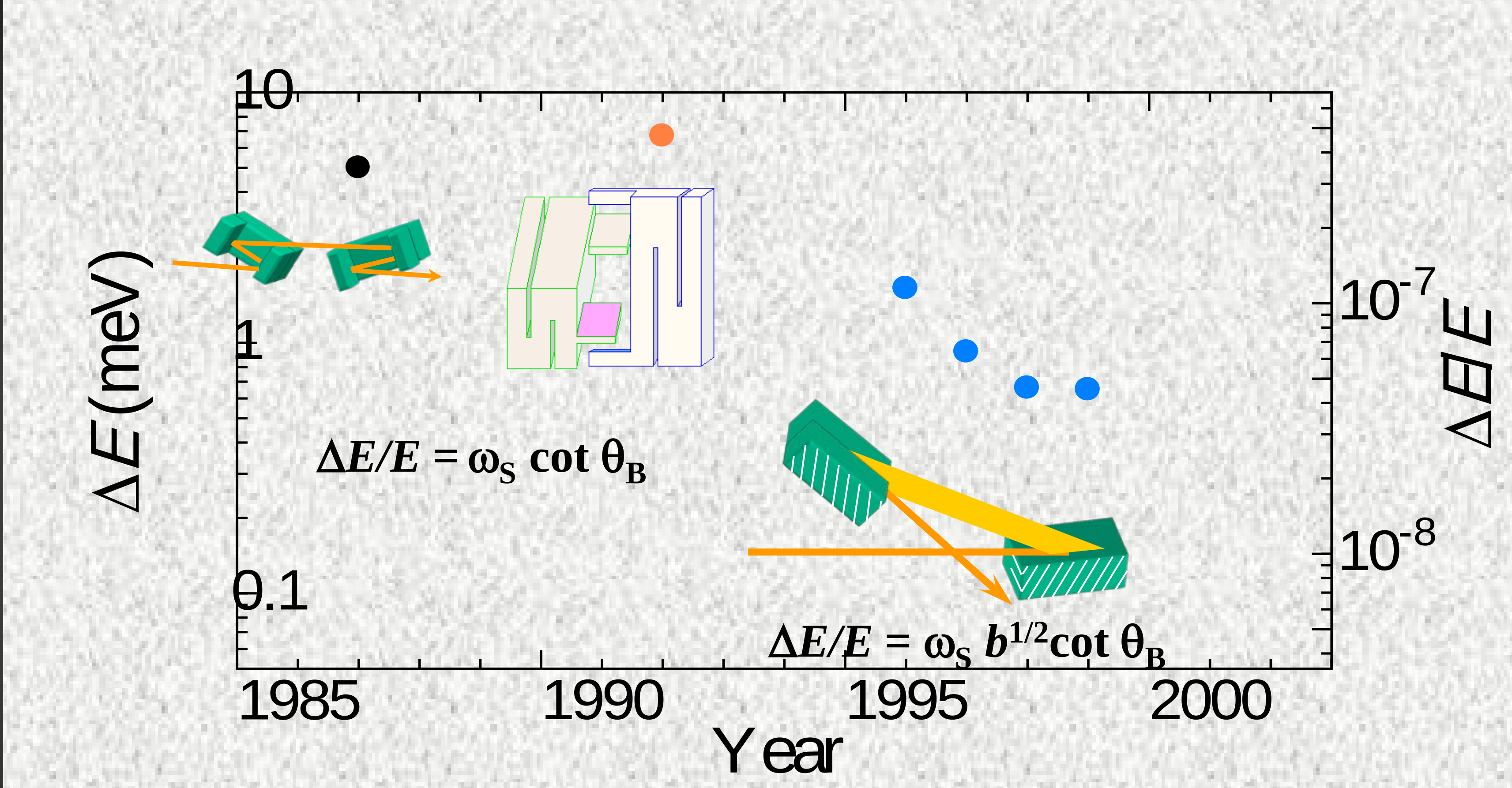

Energy Resolutions at E=14.4 keV

G. Faigel et al. 1987; T. Ishikawa et al. 1992;
T. Toellner et al. 1992, 1997; A.I. Chumakov et al. 1996, 2000

Angular Collimation with Asymmetric Reflection

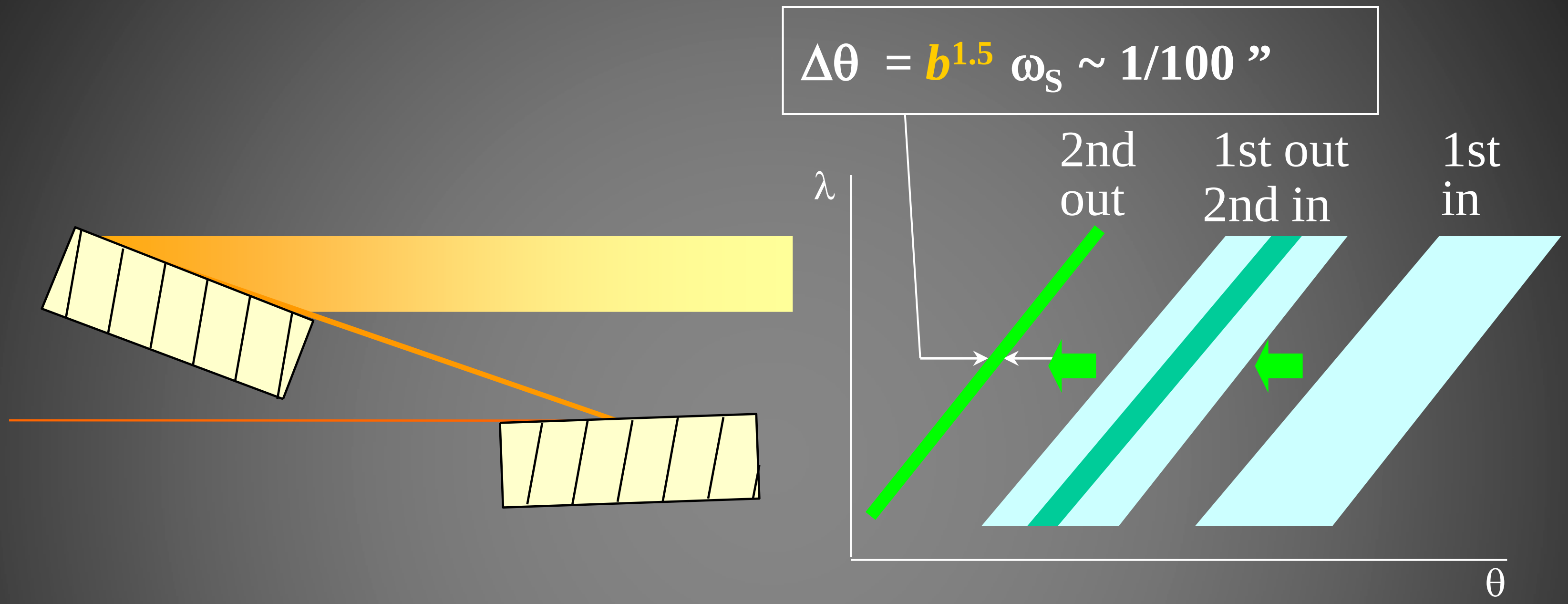

Successive asymmetric reflections in (+, –) geometry

Kohra & Kikuta, Acta A, 1968; Matsushita, Kikuta, & Kohra, JPSJ, 1971

Sub-meV Resolution HRM

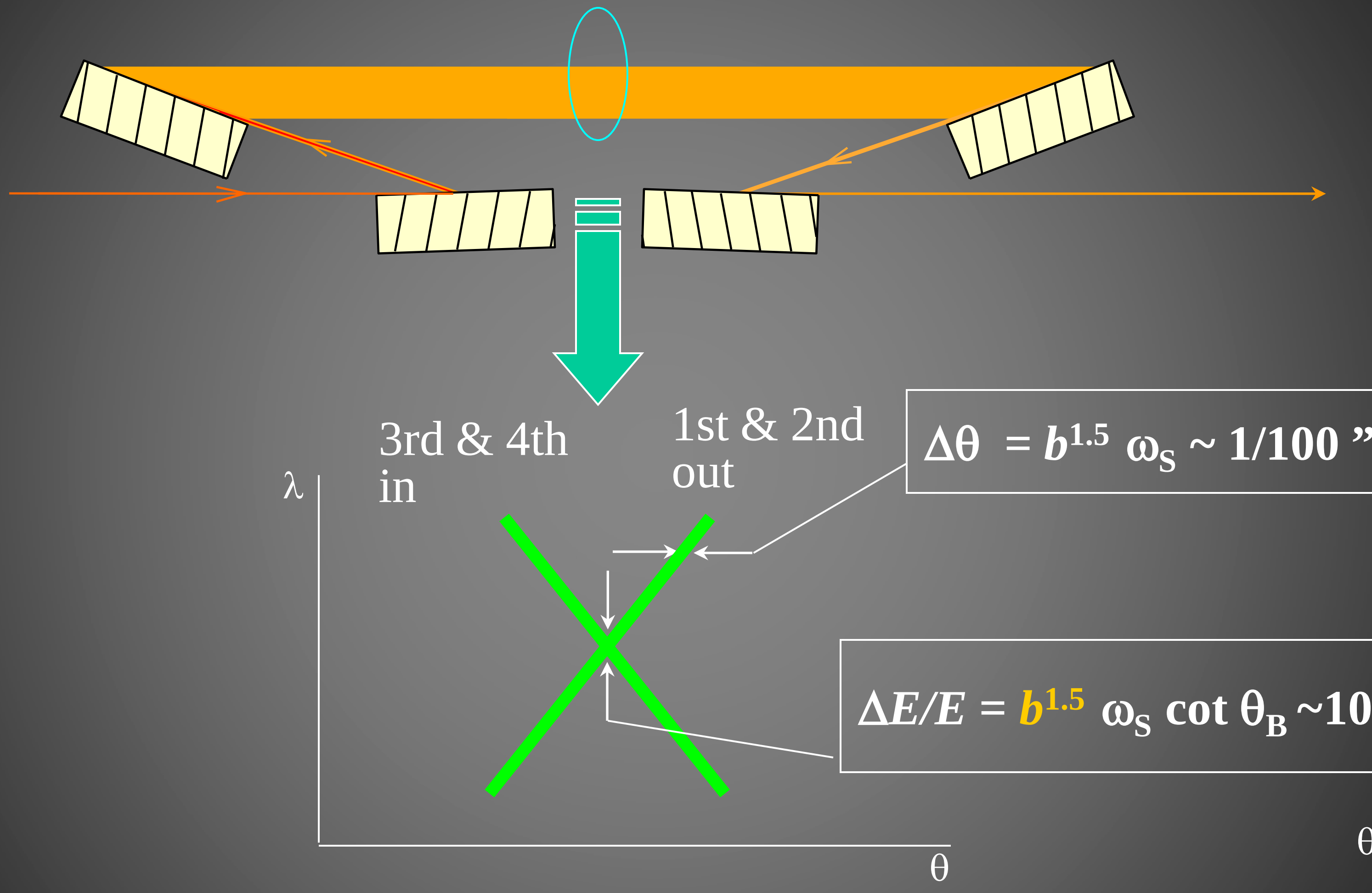

$\Delta\theta = b^{1.5}\ \omega_S \sim 1/100$ ”

$\Delta E/E = b^{1.5}\ \omega_S \cot\theta_B \sim 10^{-8}$

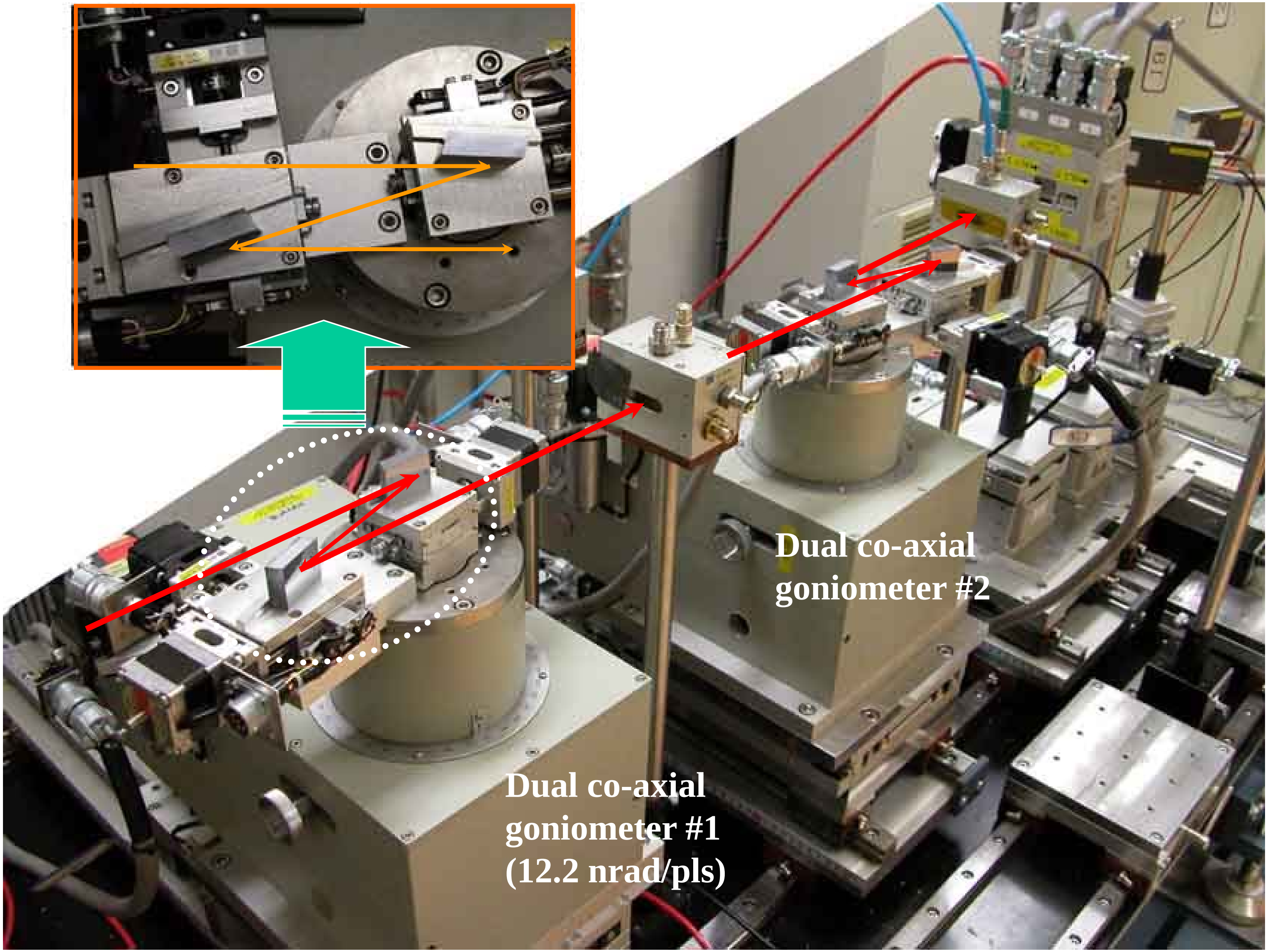
Dual co-axial
goniometer #2
Dual co-axial
goniometer #1
(12.2 nrad/pls)

Sub-meV Resolution Monochromator

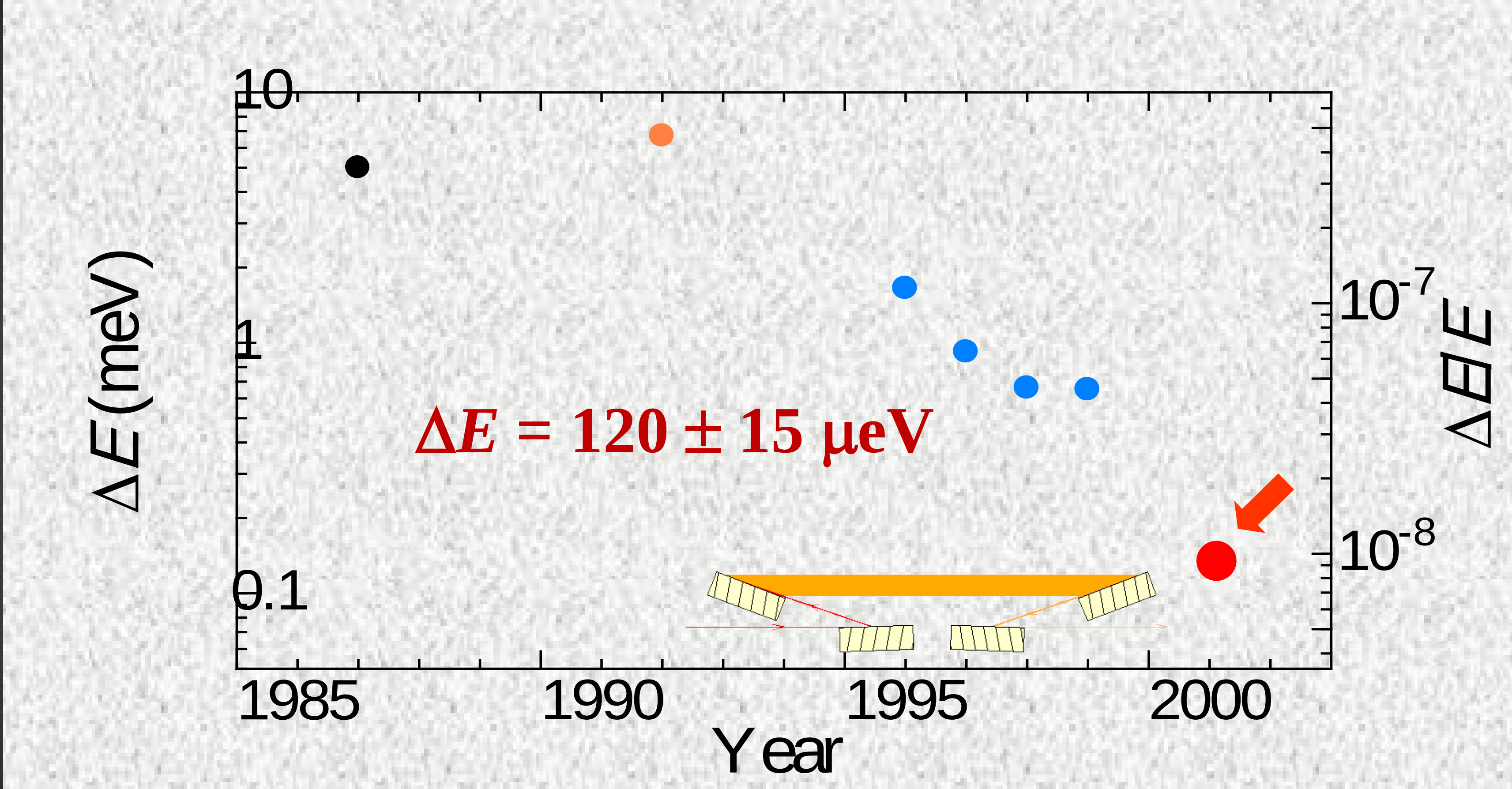

M. Yabashi, K. Tamasaku, S. Kikuta, & T. Ishikawa: RSI ***72****, 4080 (2001).*

High Brilliant Light Source: 27m ID

In-vacuum undulator
Total magnet length = 25 m
λ_U= 32 mm
N = 780
$K \leq 1.76$
E_{1st}: 7.2 ~ 18.7 keV
Total Power ≤ 35 kW
$\delta \leq 0.7$

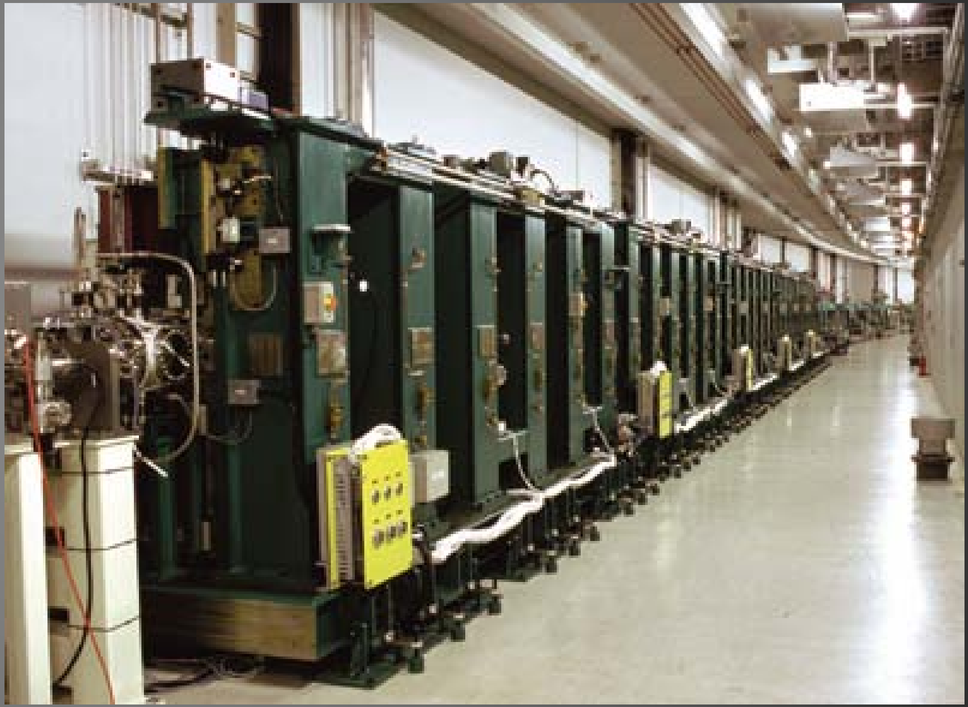

*Kitamura et al.: NIM A **467-468**, 110 (2001).*

Peak Brilliance

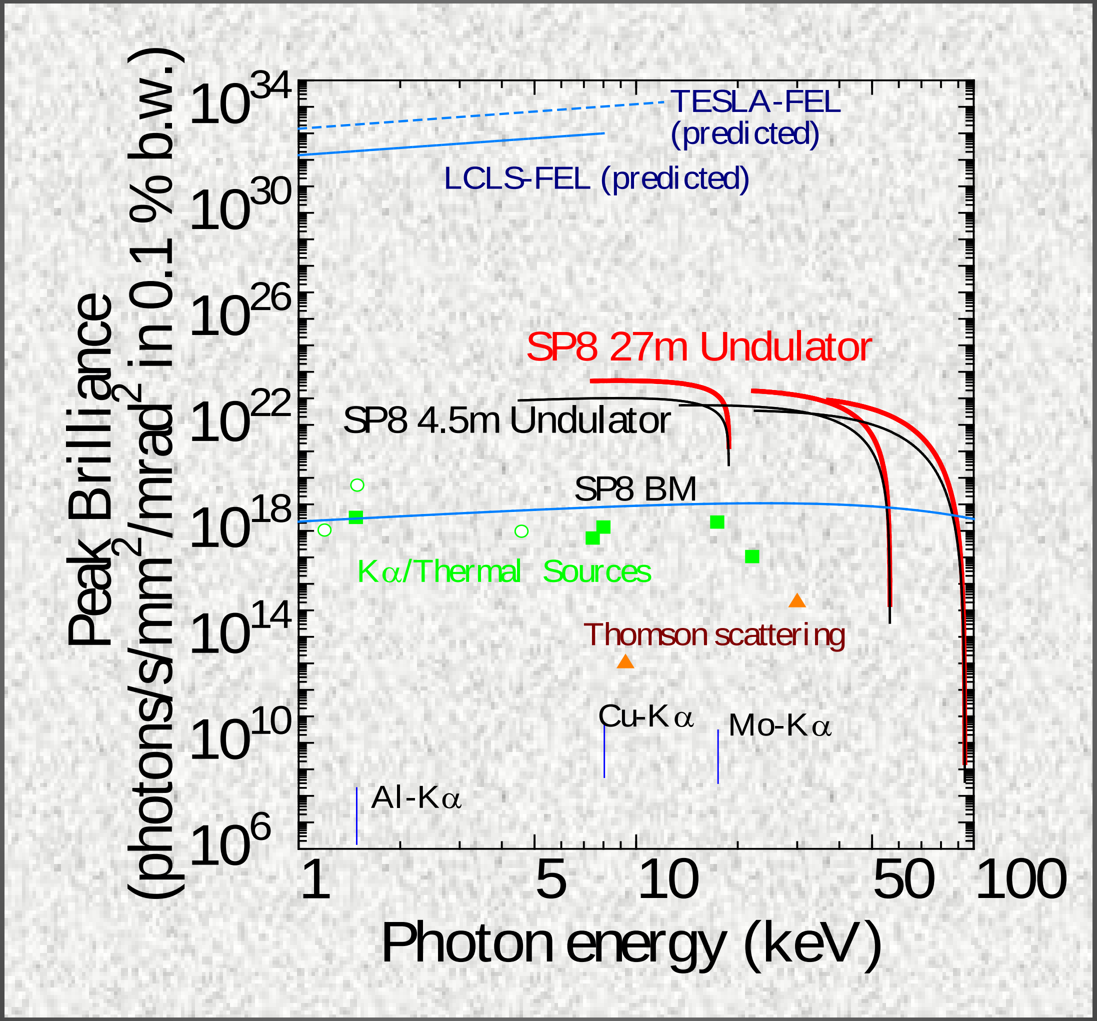

Optical Set-Up

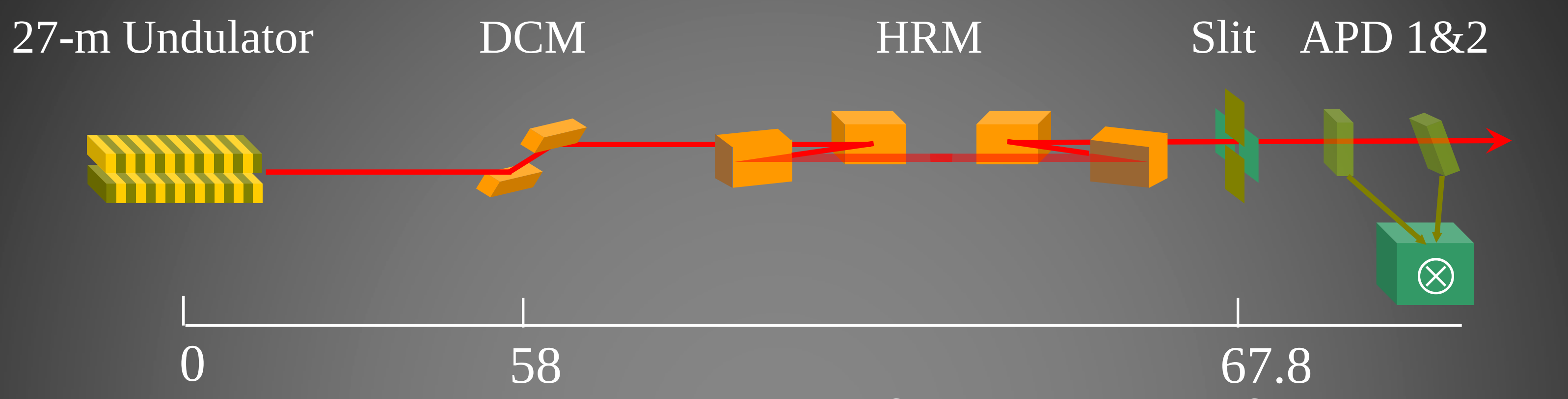

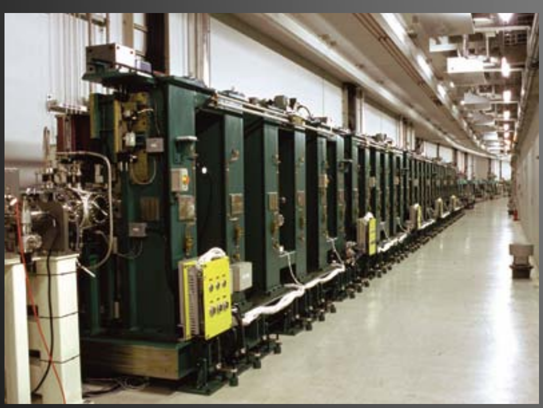

Kitamura et al., NIM A, 2001

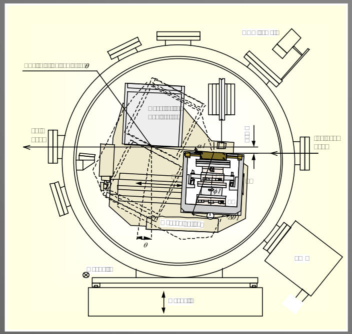

Yabashi et al., SPIE 1999;
Tamasaku et al., SPIE 2002,

Result

Horizontal slit width = 30 μm

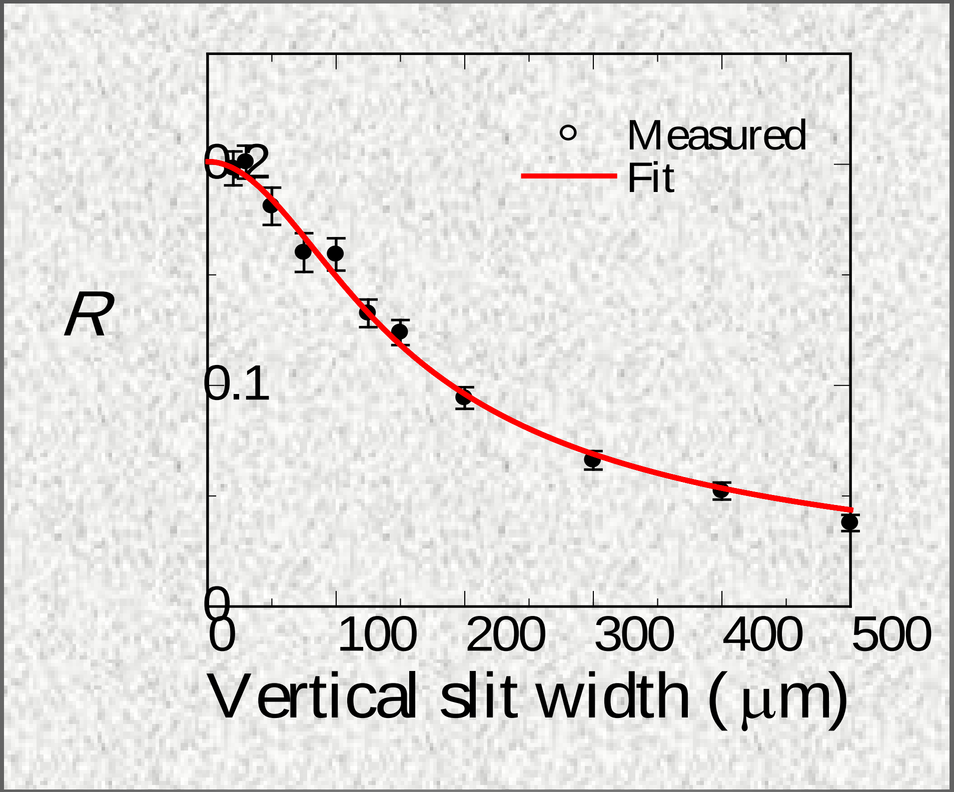

Coherence length: **σ_y = 66.3 ± 2.0 μm at *L* = 66.7 m**

Electron Beam Diagnostics

Van Cittert-Zernike's theorem (Gaussian approximation):

$\sigma_Y = \lambda L / 2\pi s_Y$

Vertical source size: $s_Y = 13.8 \pm 0.4\ \mu m$

(Angular source size: 0.2 μrad)

M. Yabashi, K. Tamasaku, and T. Ishikawa,

Phys. Rev. Lett. ***87****, 140801 (2001)*

Vertical emittance:

$\varepsilon_Y = s_Y^2 / \beta_Y$

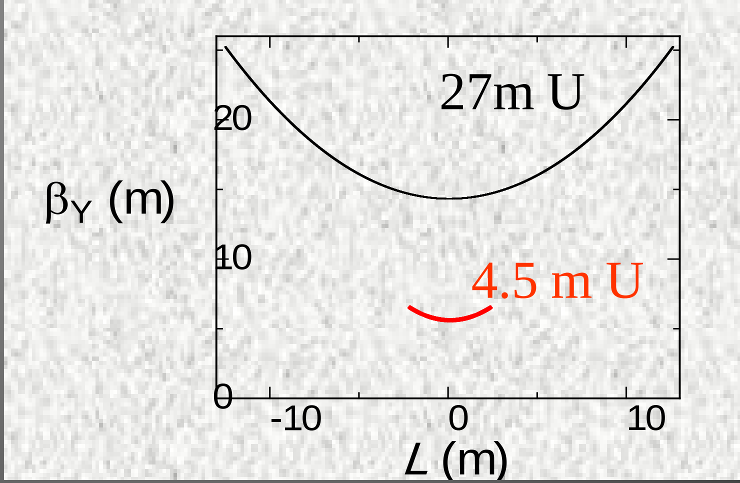

SP8 Standard 4.5 m Undulator

Measured at 1st hutch (~50 m from source) of 1-km BL

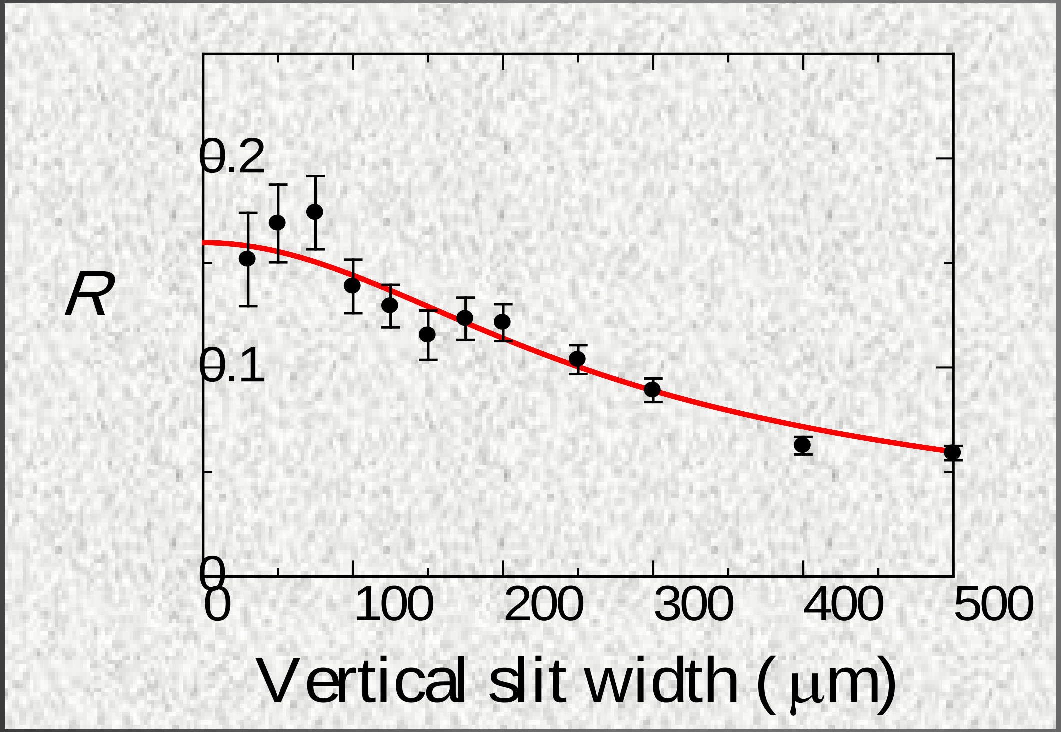

σ_y = 124.3 ± 6.9 μm
s_y = 5.9 ± 0.3 μm
ε_y = 6.0 ± 0.7 pm.rad
κ = 0.10 %

Low Emittance Operation

ε = 6 nm.rad

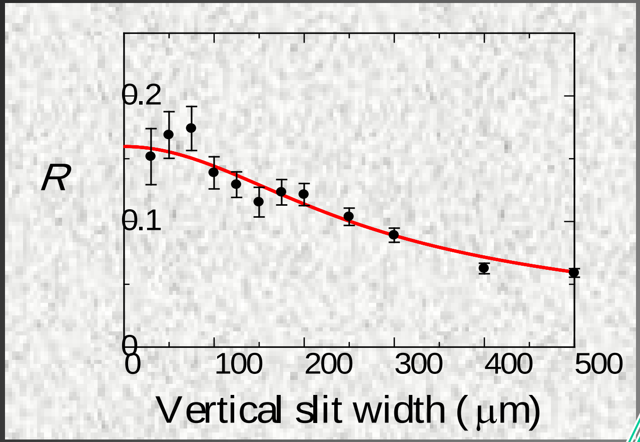

σ_y = 124.3 ± 6.9 μm
s_y = 5.9 ± 0.3 μm
ε_y = 6.0 ± 0.7 pm.rad
κ = 0.10 %

ε = 3 nm.rad

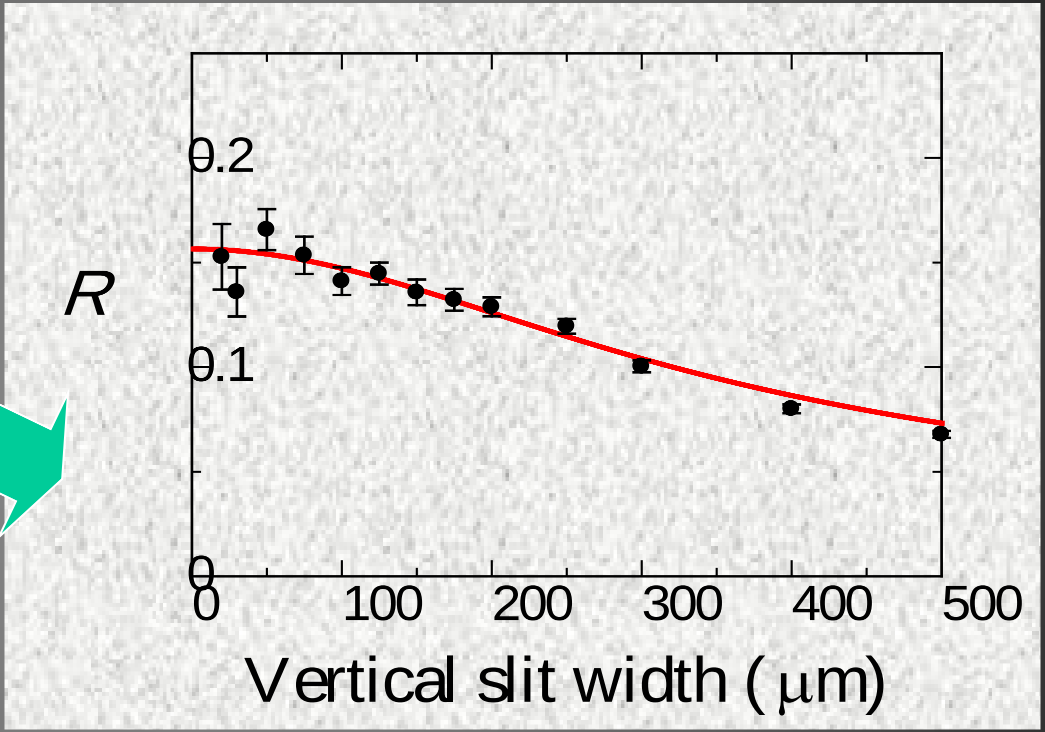

σ_y = 161.3 ± 5.0 μm, s_y = 4.6 ± 0.14 μm
ε_y = 3.6 ± 0.2 pm.rad, κ = 0.12 %

M. Yabashi, K. Tamasaku, & T. Ishikawa: PRA

Pulse Width

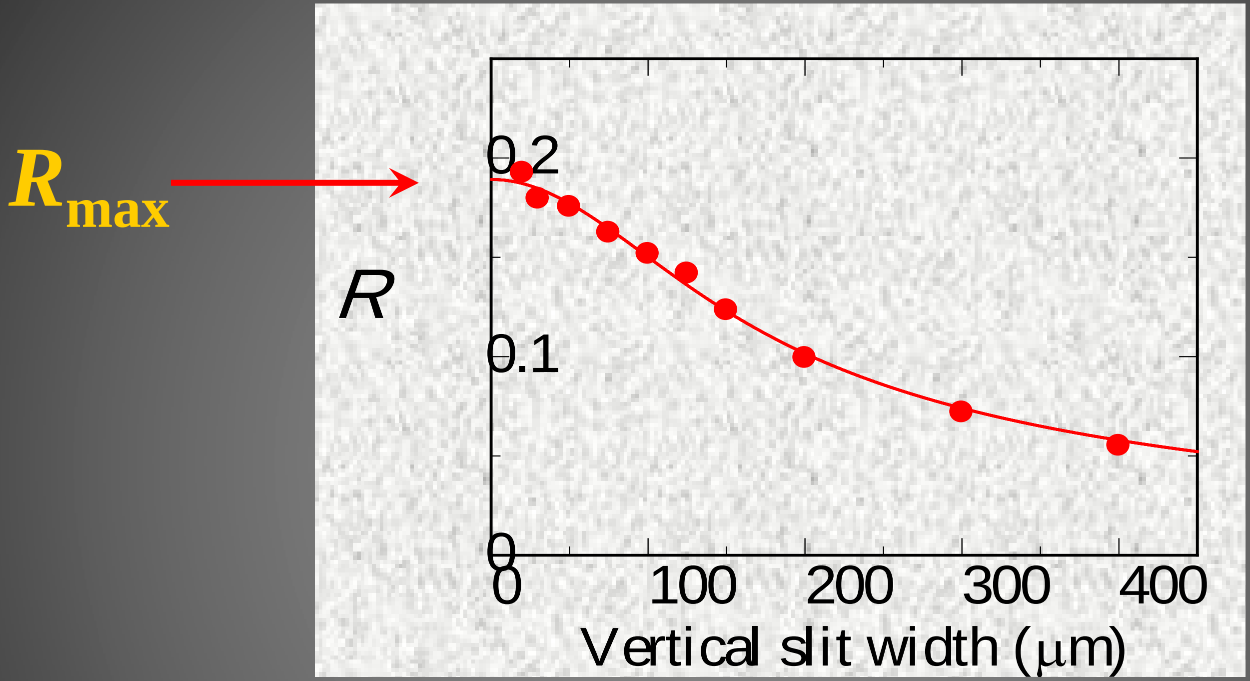

$R_{max} = 1/\,M_T = (1+ \sigma_T^{\,2} / s_T^{\,2})^{-1/2}$

$(M_X = M_Y = 1)$

$\sigma_T = 4h\ln2/\Delta E$

⇨ Pulse width s_T

σ_t is tunable through ΔE

$$\Delta E/E = \omega_S\, b^{1.5} \cot \theta_B$$

b: Asymmetric Factor

E = 14.412 keV, $1/b$ = 10
ΔE = 0.1 meV

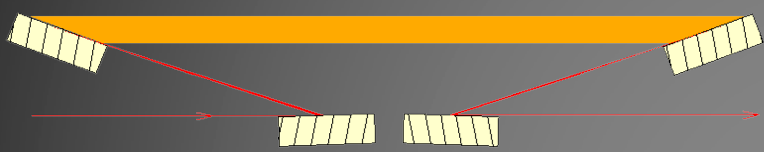

E = 14.267 keV, $1/b$ = 2.5,
ΔE = 0.76 meV

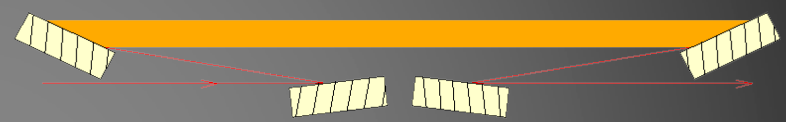

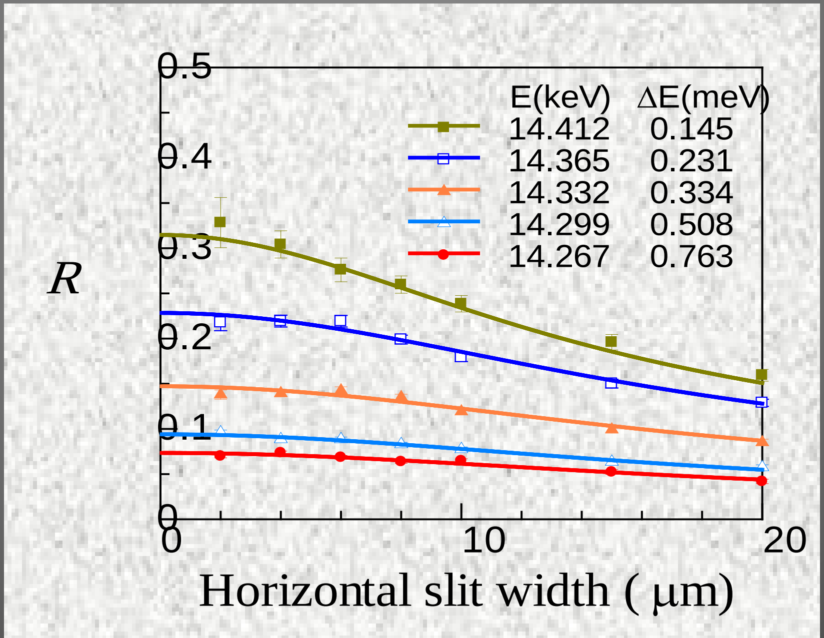

Result

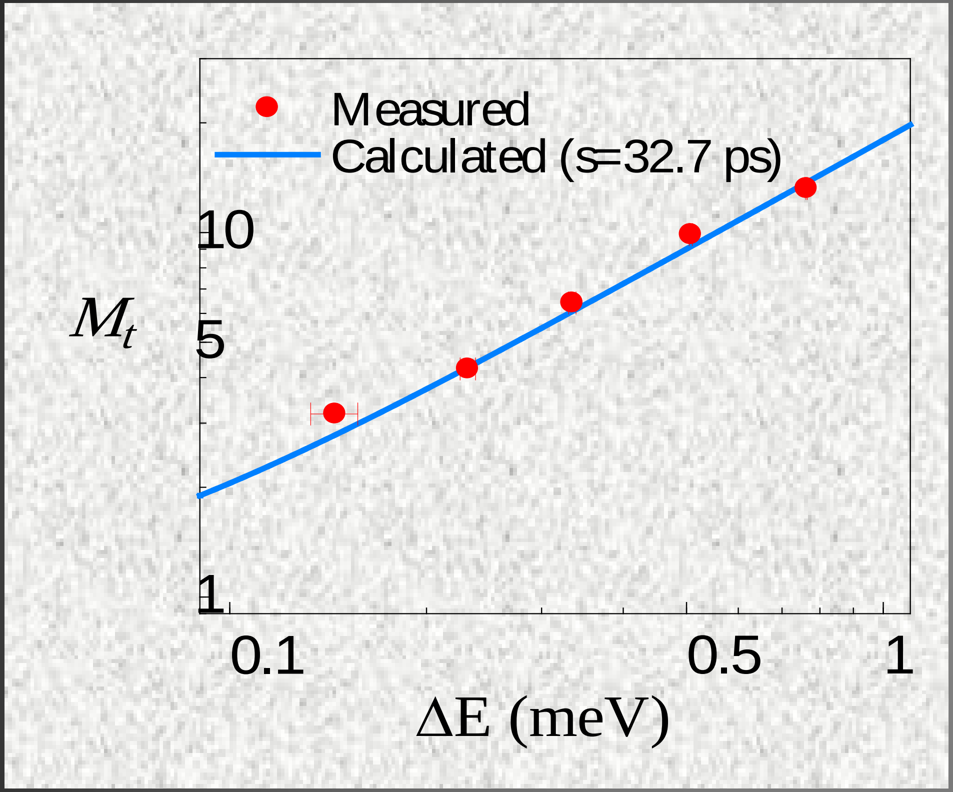

s_T = 32.7 ±1.6 ps

(Streak camera: 32 ps)

M. Yabashi, K. Tamasaku, & T. Ishikawa: Phys. Rev. Lett. ***88****, 244801 (2002).*

Intensity correlation technique is useful for amplitude interferometers

K.Tamasaku *et al.*, PRL**88**, 044801 (2002).

Monolithic type

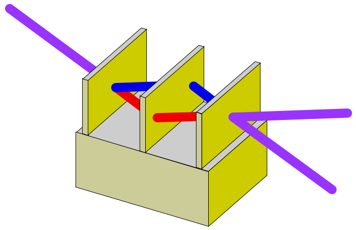

Multi-crystal type

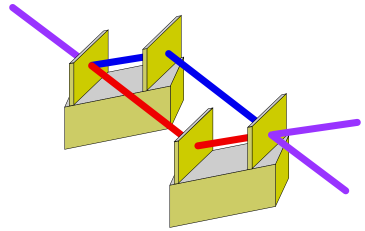

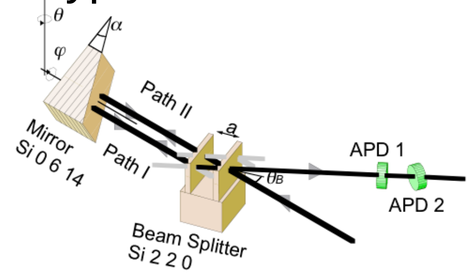

Advantage of multi-crystal interferometer:

●Large interferometer & large sample

●Flexible configuration *e.g.* use of different netplanes

But, serious drawback:

◆nano-radian/angstrome stability

Intensity correlation technique:
a novel method to measure visibility without stabilization

Fluctuating output due to instability

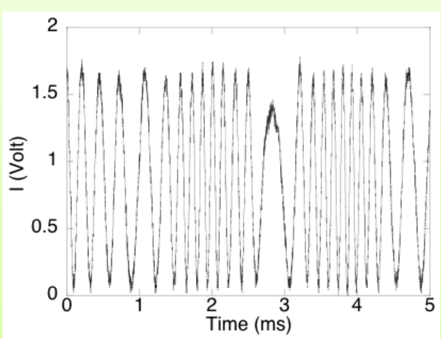

$$I(t) = \langle I \rangle (1 + V\cos\phi(t)) \Rightarrow \langle I^2 \rangle = \langle I \rangle^2 (1 + V^2)$$

If we measure the intensity correlation, $<I^2>$, we can determine the visibility, *V*.

Skew symmetric LLL interferometer

K.Tamasaku *et al.*, PRL**88**, 044801 (2002).

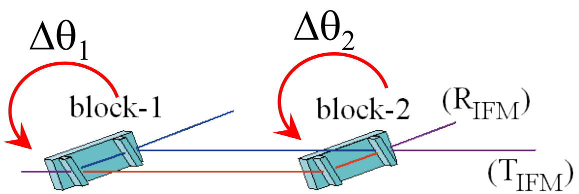

Intensity correlation: $P_{12}=1+V^2$

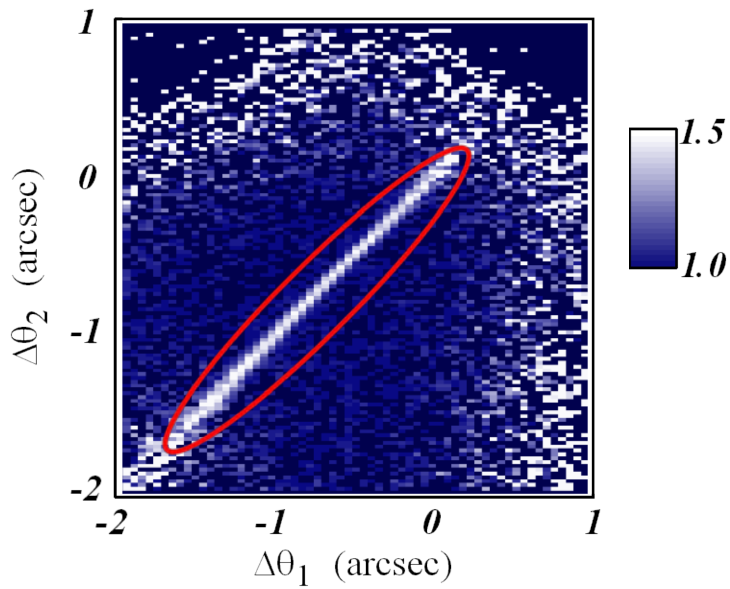

T_{IFM}

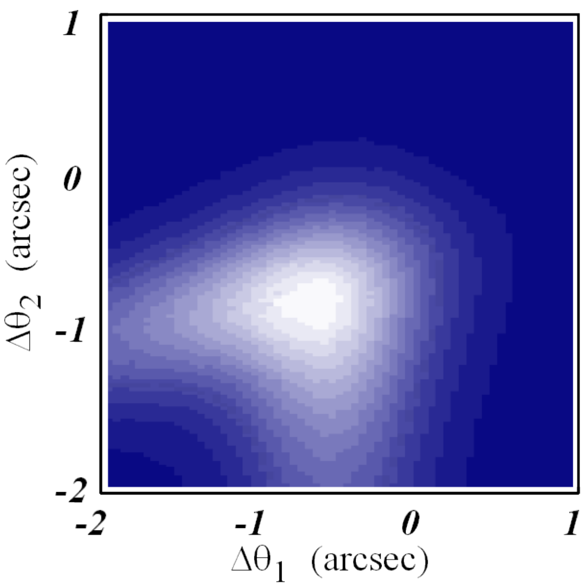

Quick measurement of P_{12} → Narrow angular range, $\Delta\theta_1=\Delta\theta_2$, is usable.

X-ray Michelson interferometer & Fourier transform x-ray spectroscopy

K.Tamasaku *et al.*, APL**83**, 2994 (2003).
K.Tamasaku *et al.*, JSR**12**, 696 (2005).

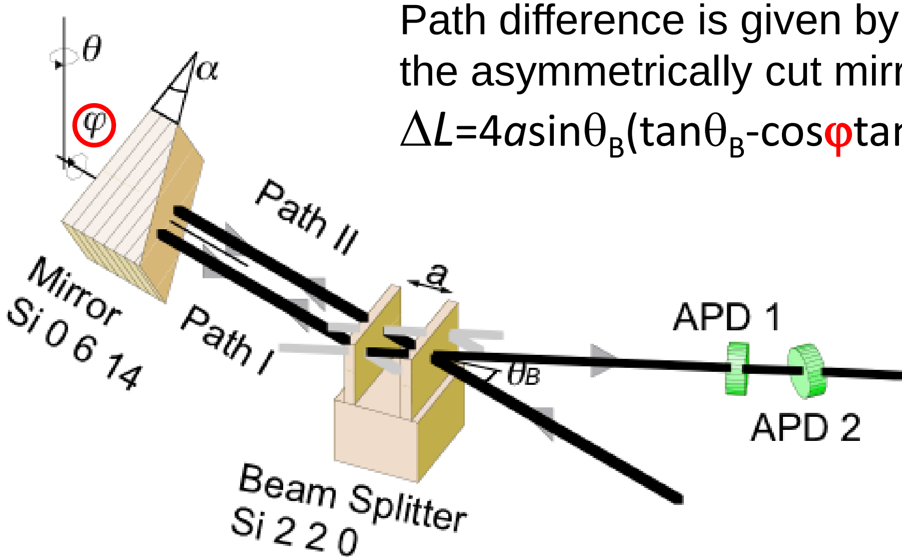

Path difference is given by rotating the asymmetrically cut mirror:
$\Delta L = 4a\sin\theta_B(\tan\theta_B - \cos\varphi\tan\alpha)$

Ultra-high resolution spectroscopy
$\Delta\lambda/\lambda \sim \lambda/\Delta L$
e.g. ΔL=100 mm, λ=1 Å: $\Delta\lambda/\lambda \sim 10^{-9}$

$P_{12}=1+V^2$

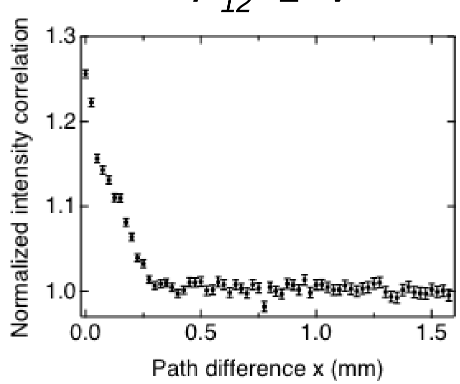

FT

Spectrum of the mirror: the 0 6 14 reflection

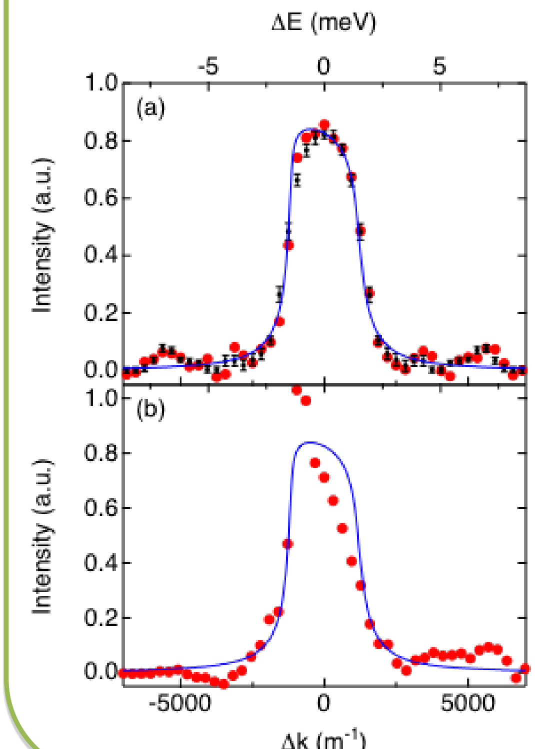

PRL 94, 174801 (2005) PHYSICAL REVIEW LETTERS week ending 6 MAY 2005

X-Ray Resonance in Crystal Cavities: Realization of Fabry-Perot Resonator for Hard X Rays

S.-L. Chang,[1,2,*] Yu. P. Stetsko,[2] M.-T. Tang,[2] Y.-R. Lee,[1] W.-H. Sun,[1] M. Yabashi,[3] and T. Ishikawa[3,4]
[1]*Department of Physics, National Tsing Hua University (NTHU), Hsinchu, Taiwan 300, Republic of China*
[2]*National Synchrotron Radiation Research Center (NSRRC), Hsinchu, Taiwan 300, Republic of China*
[3]*SPring-8/JASRI, Mikazuki, Hyogo 679-5198, Japan*
[4]*SPring-8/RIKEN, Mikazuki, Hyogo 679-5148, Japan*
(Received 9 August 2004; published 5 May 2005)

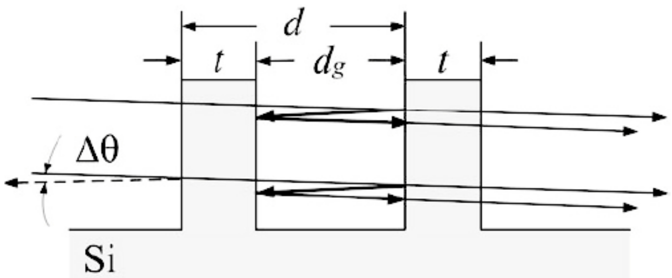

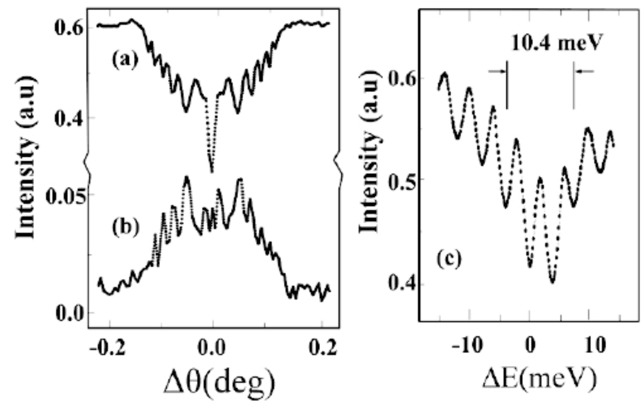

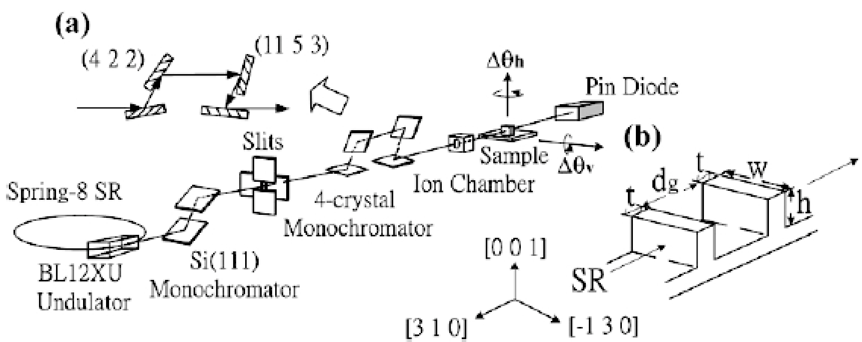

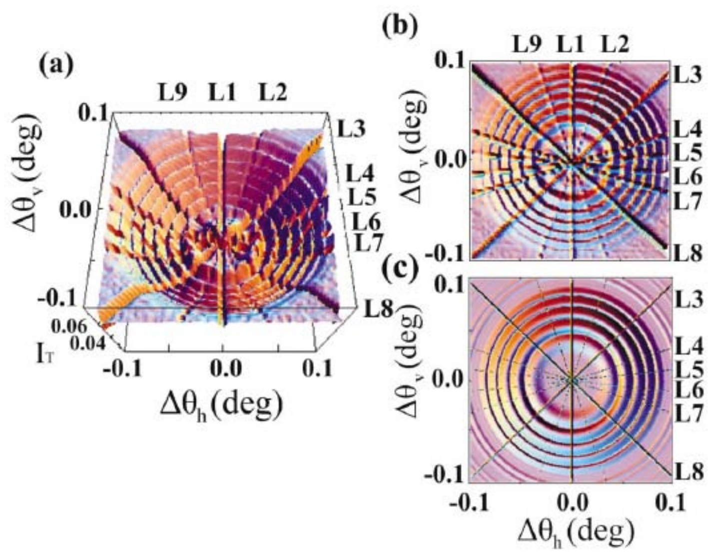

X-ray nonlinear optics – x-ray PDC

K.Tamasaku *et al.*, PRL**98**, 244801 (2007).

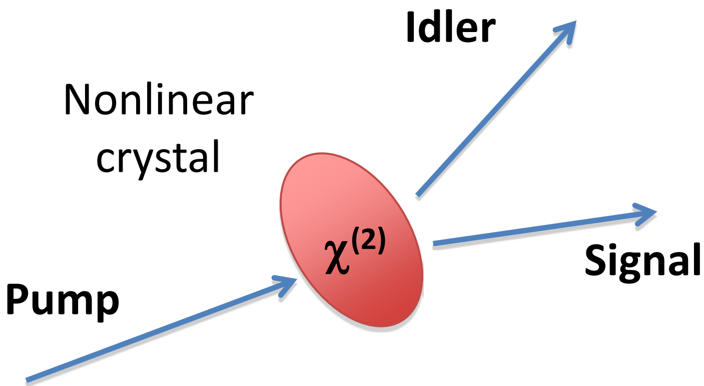

X-ray PDC (parametric down-conversion):

the 2nd order nonlinear optical process accessible with existing SR

The pump photon decays spontaneously into two photons, the idler and the signal.

- Energy conservation: $\omega_p=\omega_s+\omega_i$
- Momentum conservation: k_p+Q=k_s+k_i

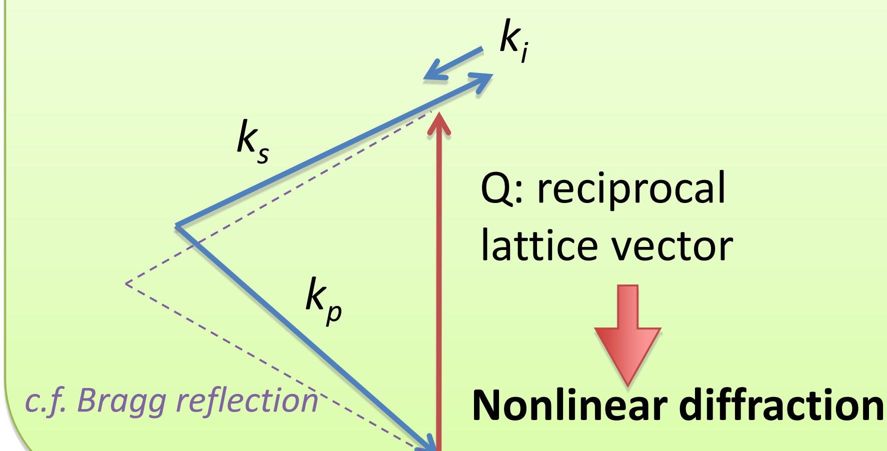

Basic questions

- How x-ray PDC is observed?
- How to estimate $\chi^{(2)}$?
- What factor determines $\chi^{(2)}$?

$\chi^{(2)}$: nonlinear susceptibility

X→X+SX by diamond

K.Tamasaku *et al.*, PRL**103**, 254801 (2009).

Exp. condition
Pump: 9.67 keV
Idler: 278-343 eV
Q=(2,2,0)

Schematic energy diagram

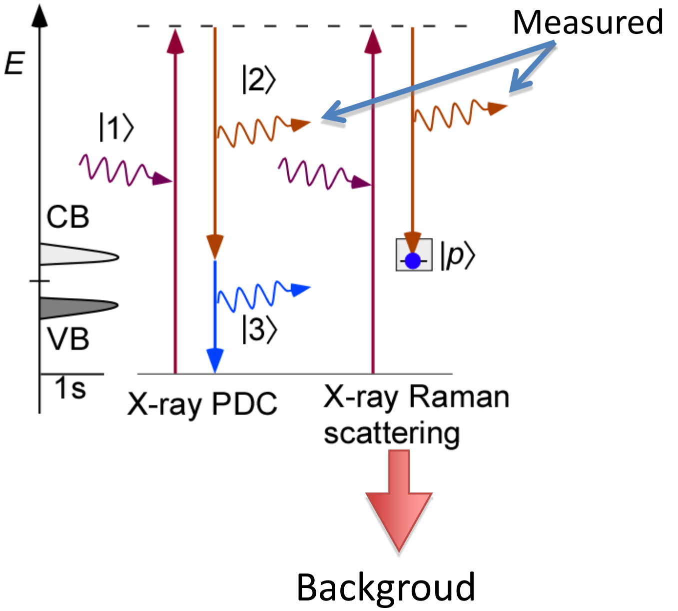

Rocking curve of nonlinear diffraction:
normalized intensity of the signal wave

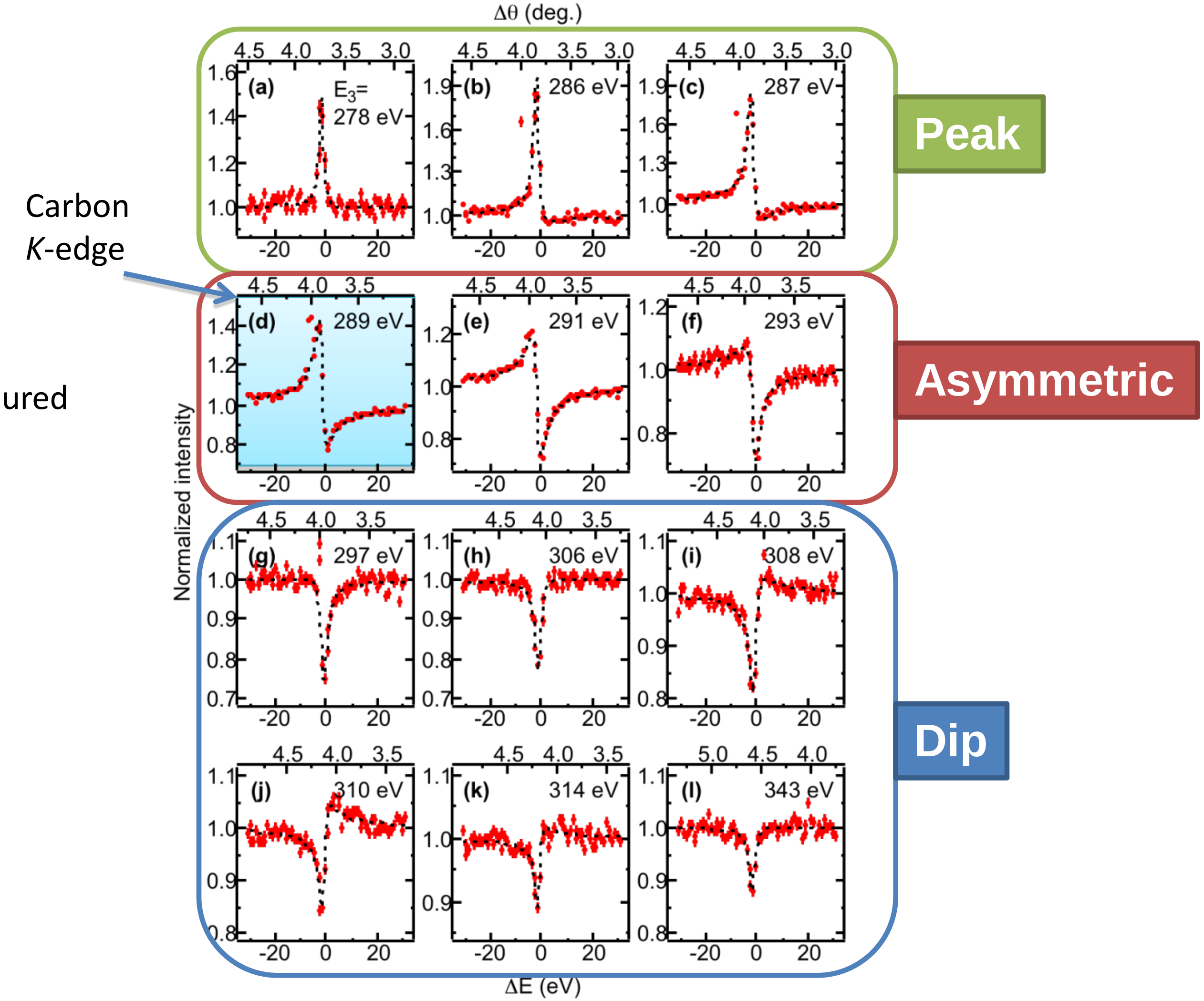

RC is not simple, but shows an interference with the background Raman process.

Resonance effect & Fano interference

K.Tamasaku *et al.*, PRL**103**, 254801 (2009).

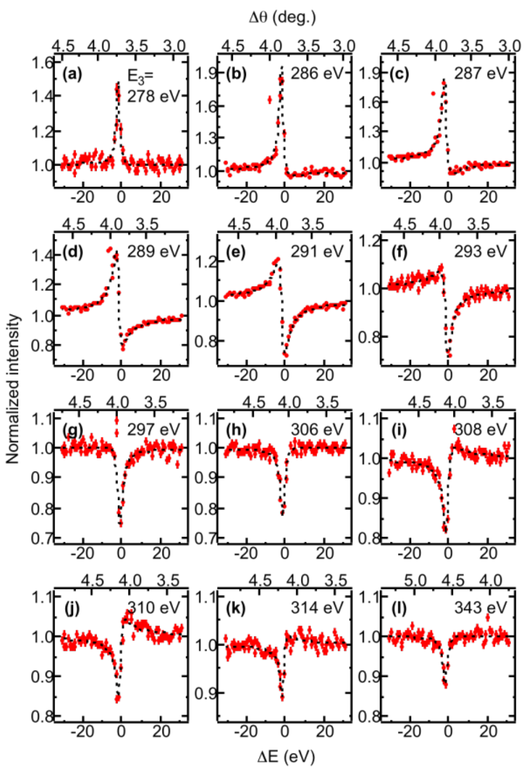

Fano picture

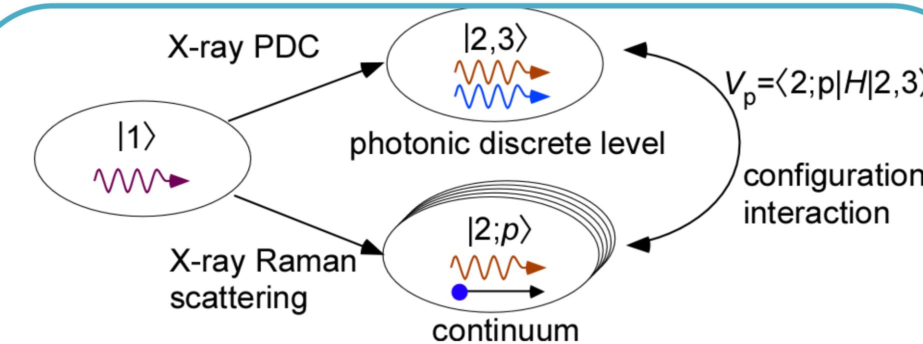

Quantum mechanical interference,
because we cannot specify which process produced the measured x-ray photon.

Analysis based on the Fano picture

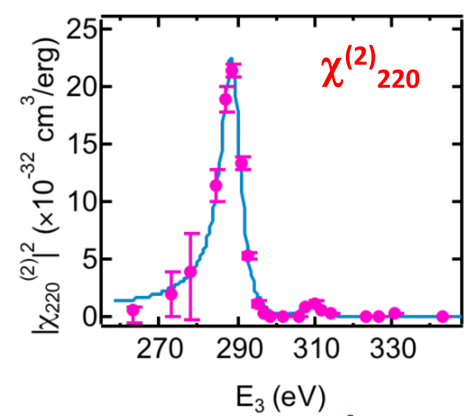

Strong resonance enhancement @ carbon K-edge

◆What factor determines $\chi^{(2)}$?

To be answered…

1000 m Beamline, BL29XUL

Great Possibility of the Coherent X-Rays

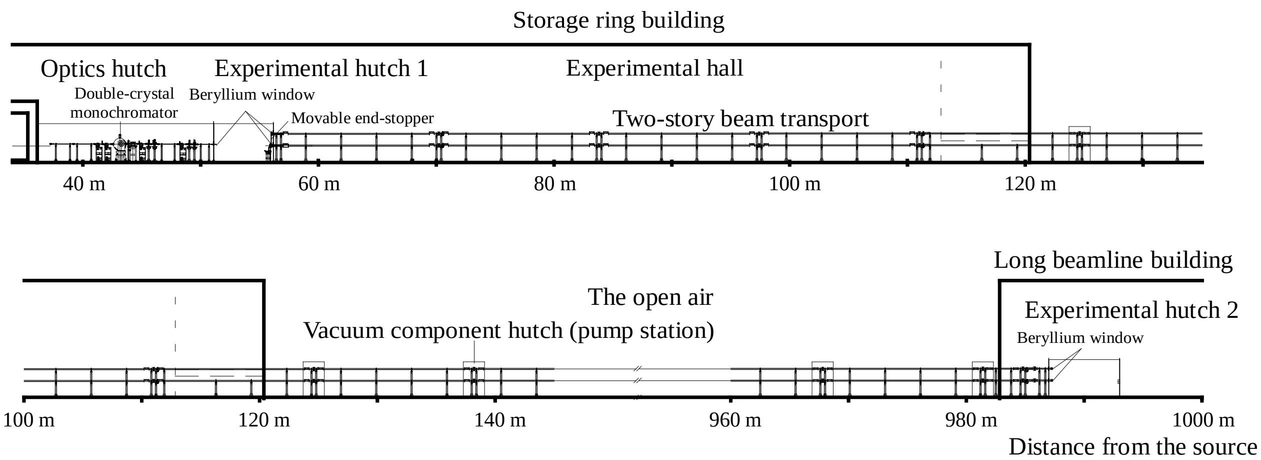

First Beam on June 2nd, 2000

from SPring-8 Homepage

First Beam at 1 km Building

June 2, 2000

SPring-8 succeeded in threading x-ray photon beam through 1 km vacuum duct on June 2, 2000, at RIKEN Physics Beamline (BL29XU). Monochromatized x-rays were guided to 1 km experimental station at 23:13, after 20 min from the start of optics alignment.

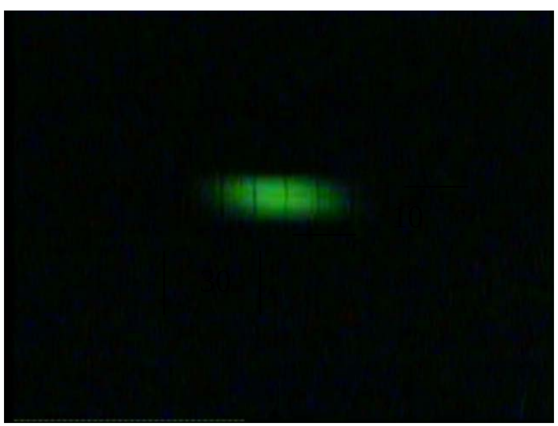

Mirror Development & Application

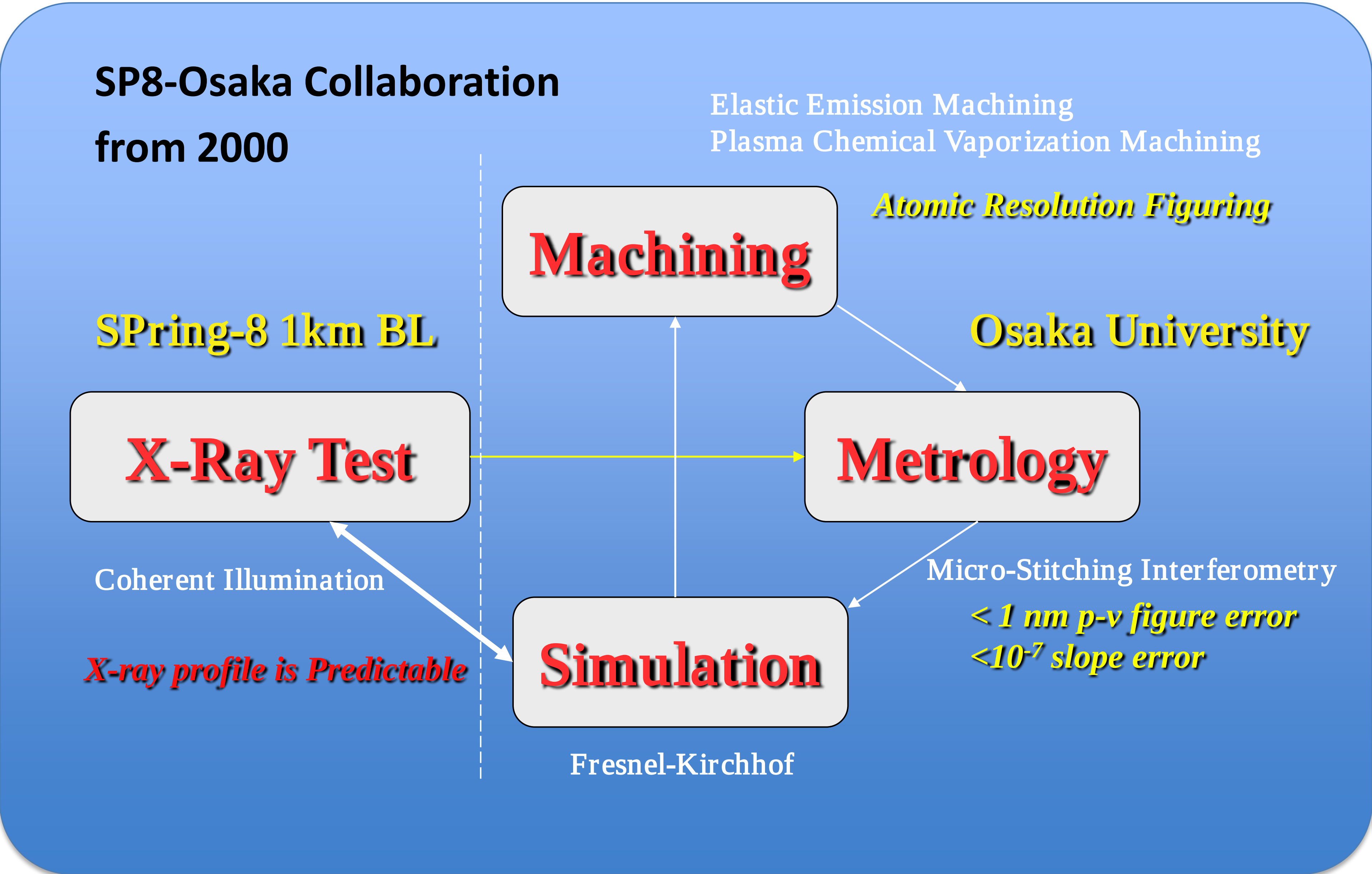

Mechanism of EEM (Elastic Emission Machining)

An ultraprecision machining process utilizing chemical reaction between surfaces of work and fine powders

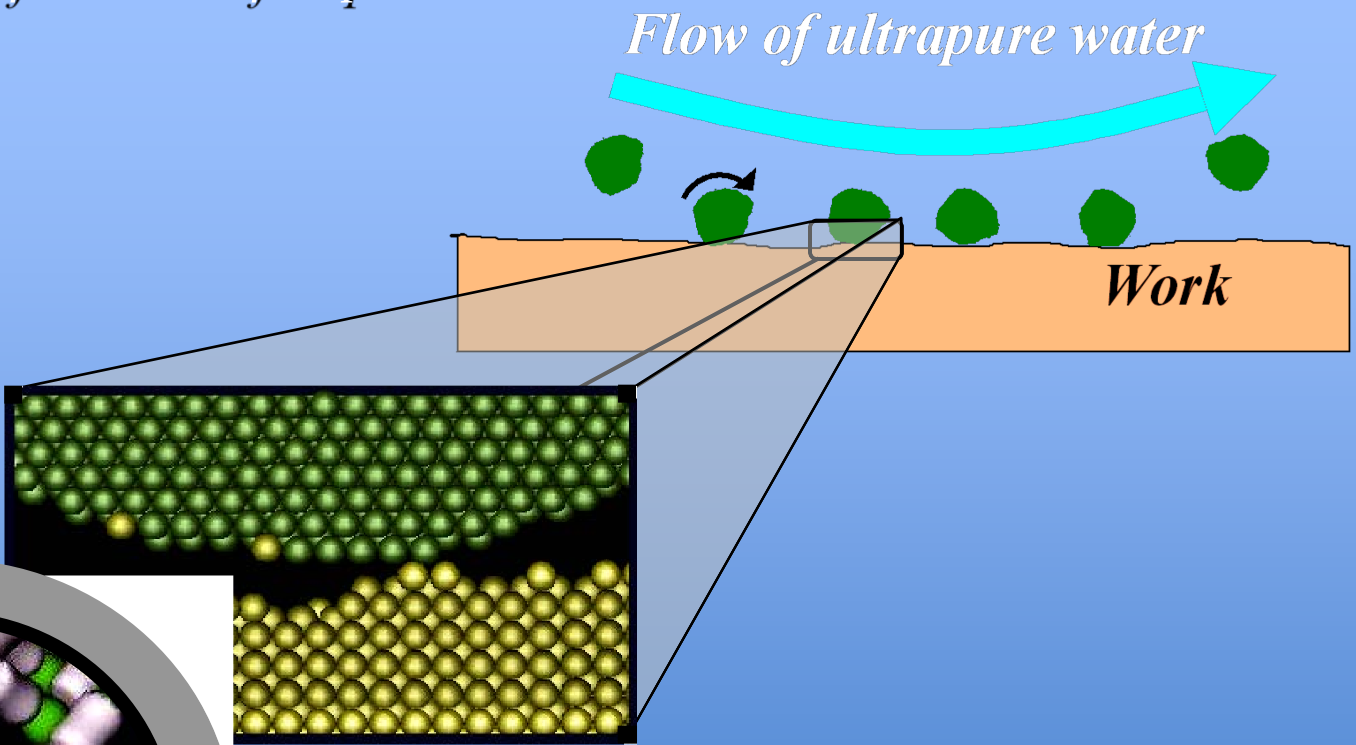

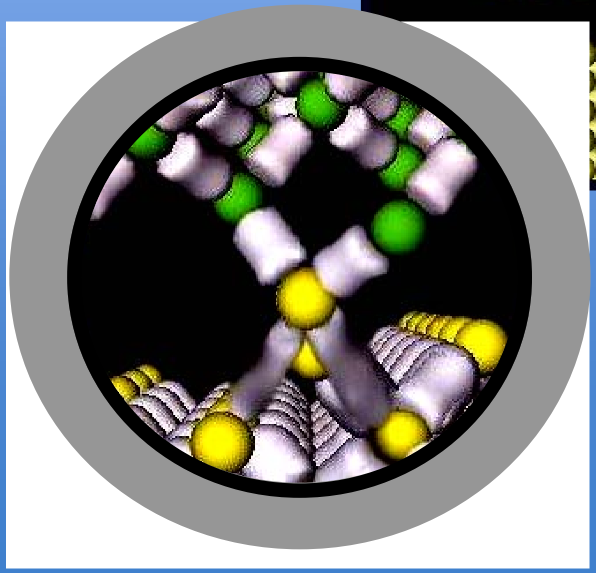

Chemical reactions are induced between only top-site atoms of the work and fine powders

⇩

Automatic smoothing mechanism

Features of Plasma CVM

1. *A chemical process utilizing reactive species generated in the atmospheric pressure plasma*

Radical density is very high.

High removal rate processing without any crystallographic damage

Material	Removal rate(μm/min)
Fused silica	170
Silicon	94
Molybdenum	36
Tungsten	32
Silicon carbide	6.4
Diamond	2.5

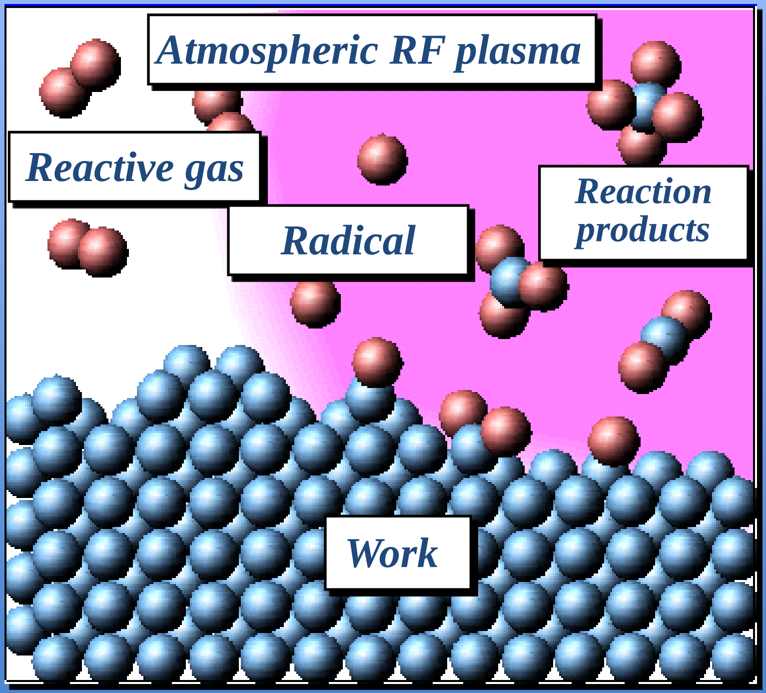

Experimental Setup

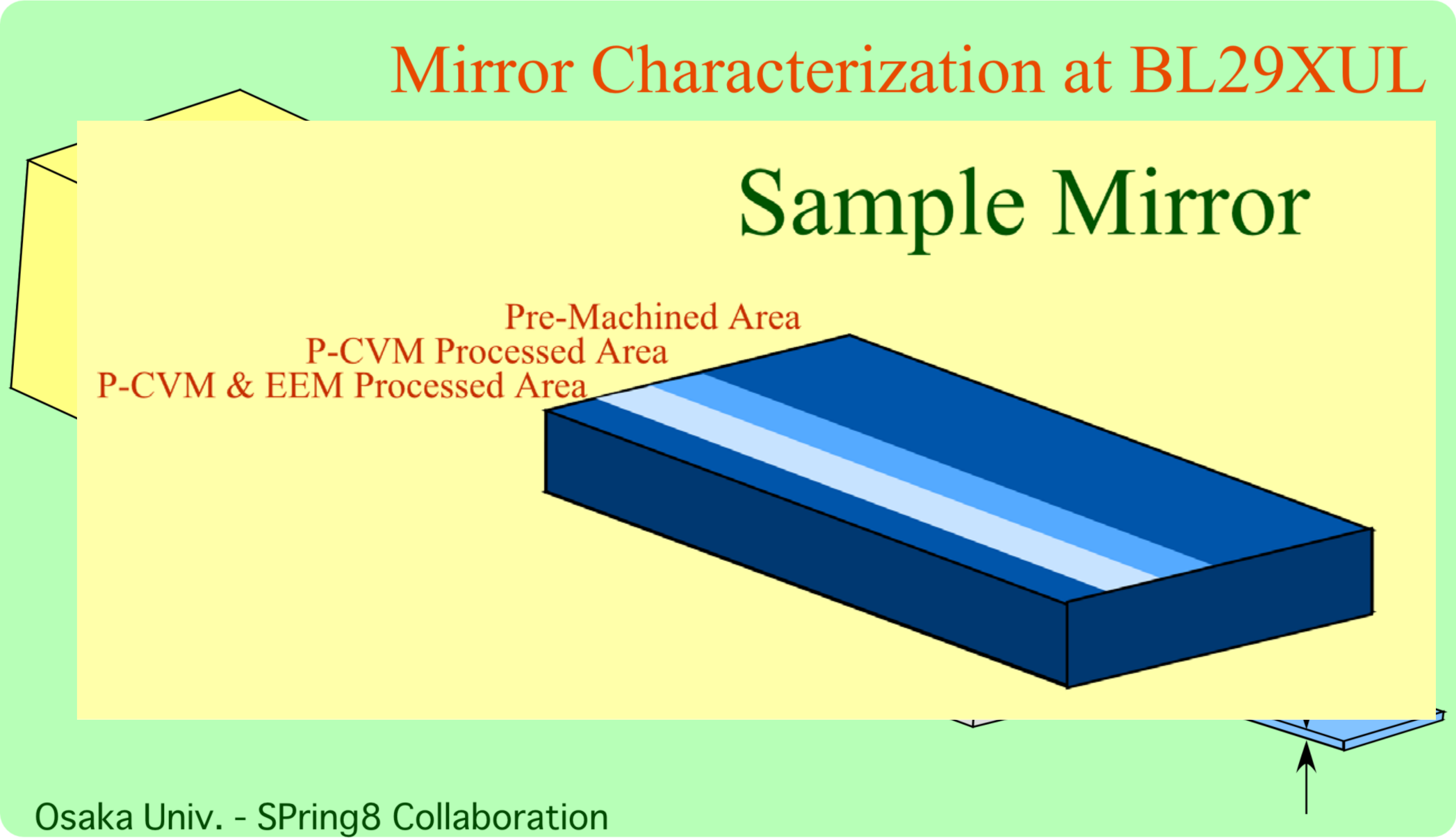

Performances of Plasma CVM Figuring

Material Single Crystal Silicon (100) ρ=1～20Ωcm
Figure Plane
Size 400 mm × 50 mm × 30 mm
（evaluated area 320 mm × 40 mm）

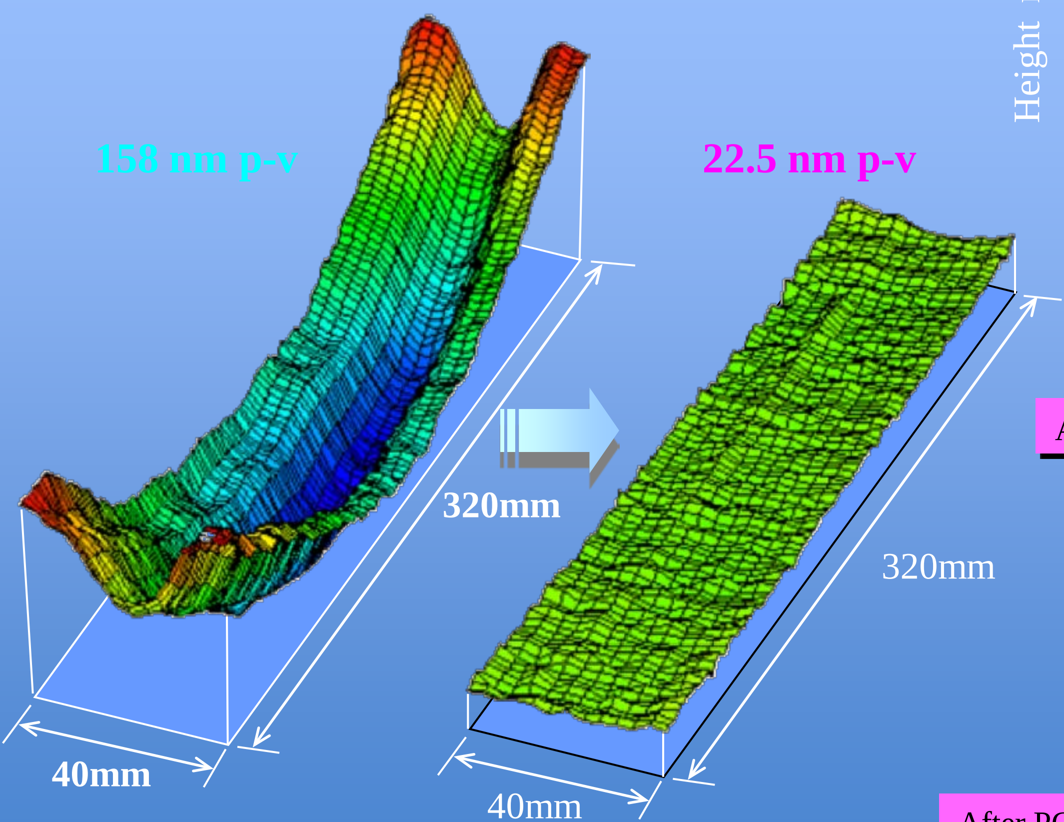

Before correction

After correction by numerically controlled plasma CVM

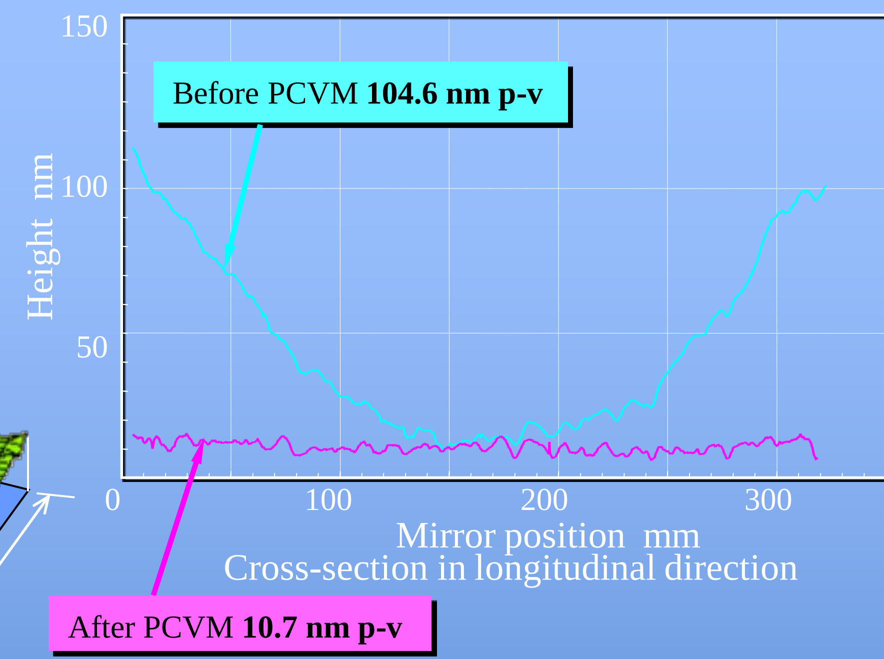

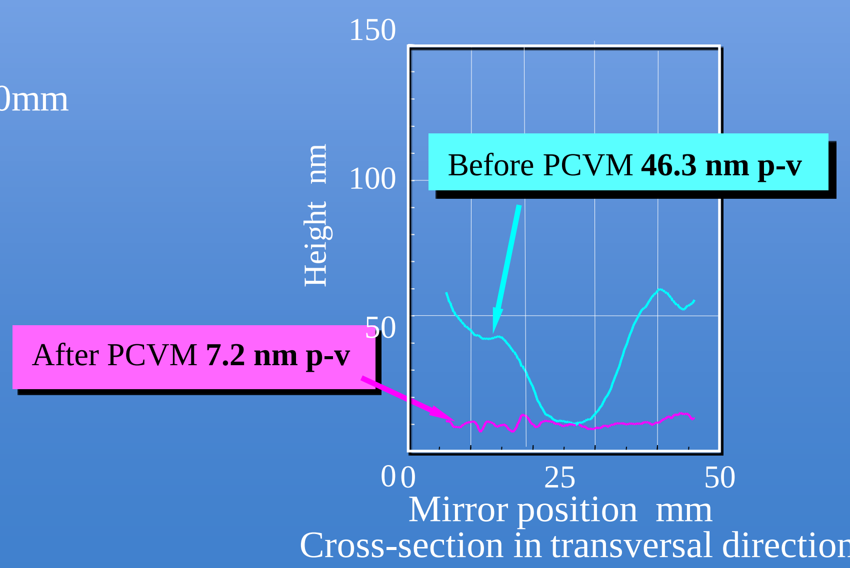

An example of the figuring in spatial-wavelength range of submillimeter by computer controlled EEM (Elastic Emission Machining) process.

Figure error：
3.5nm (p-v)
0.5nm (rms)

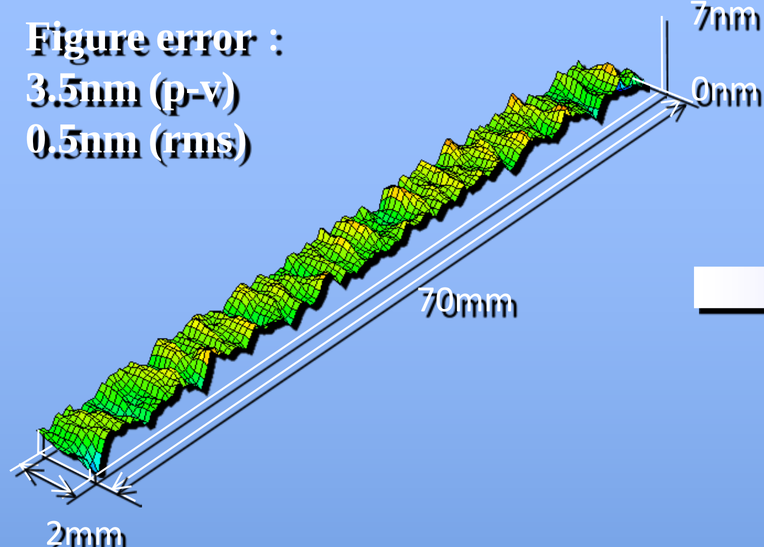

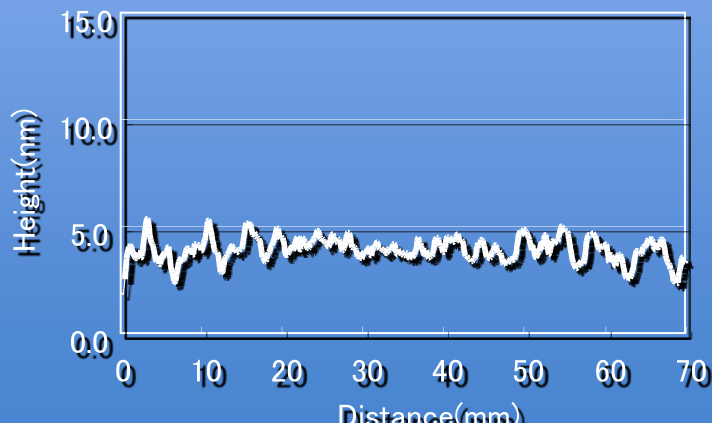

Line profile in longitudinal direction

Figure error：
2.0nm (p-v)
0.2nm (rms)

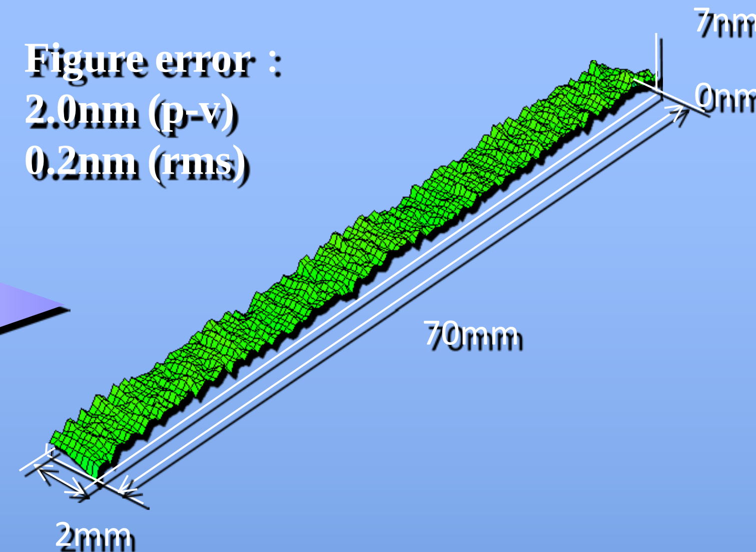

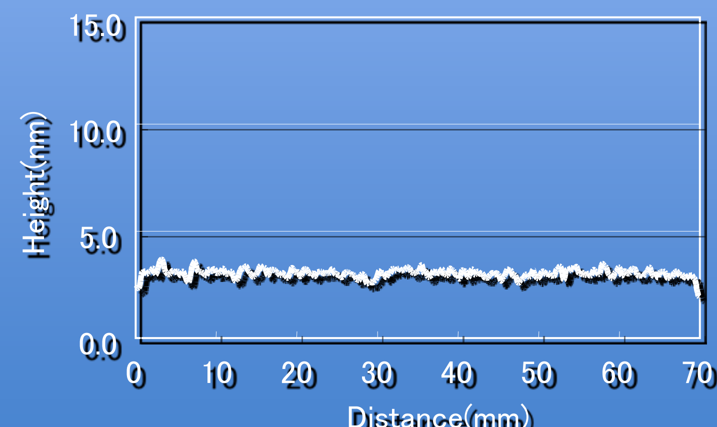

Line profile in longitudinal direction

Intensity distribution of reflected X-ray beam

Incident angle : 1.2mrad / Mirror length : 100mm / Mirror material : Silicon single crystal (001)

Camera distance: | Pre-machined surface | CVM surface | CVM+EEM surface

166mm

566mm

966mm

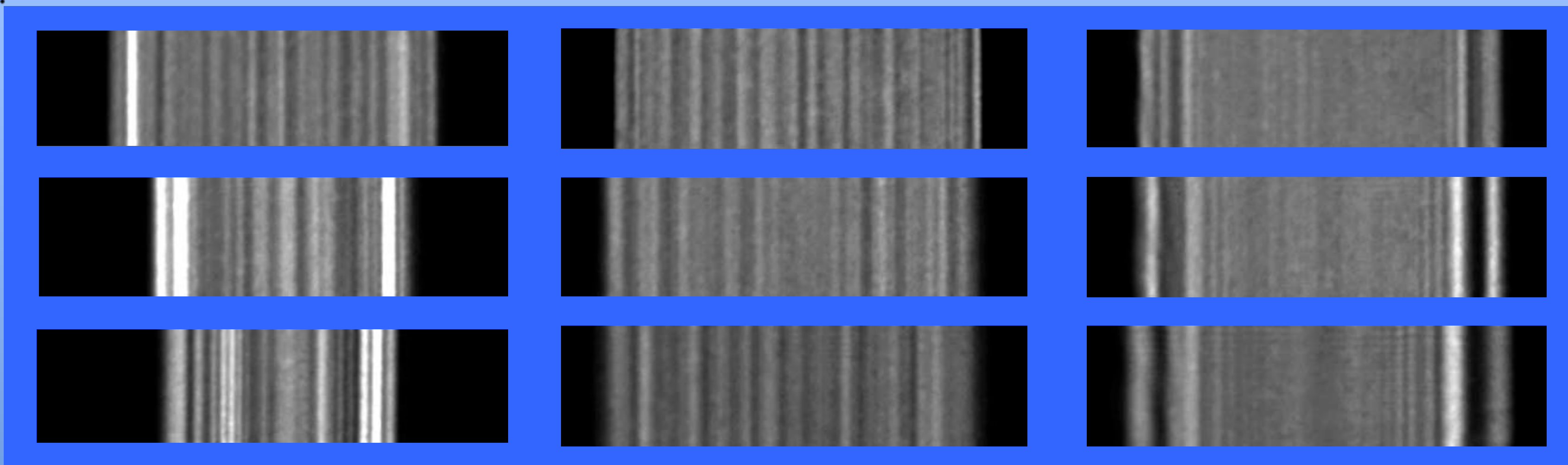

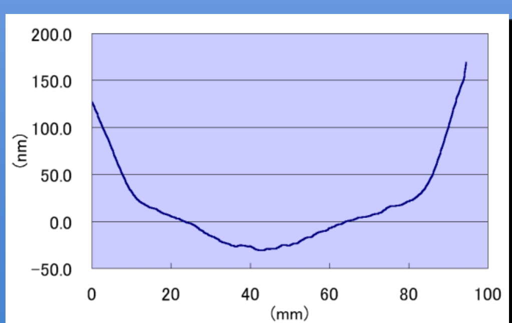

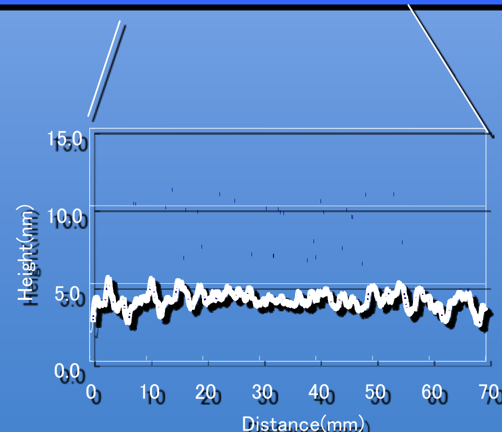

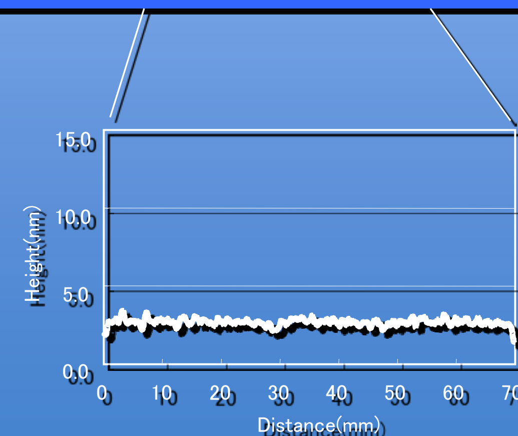

Forward/Backward Simulations

Wave-Optical Calculation

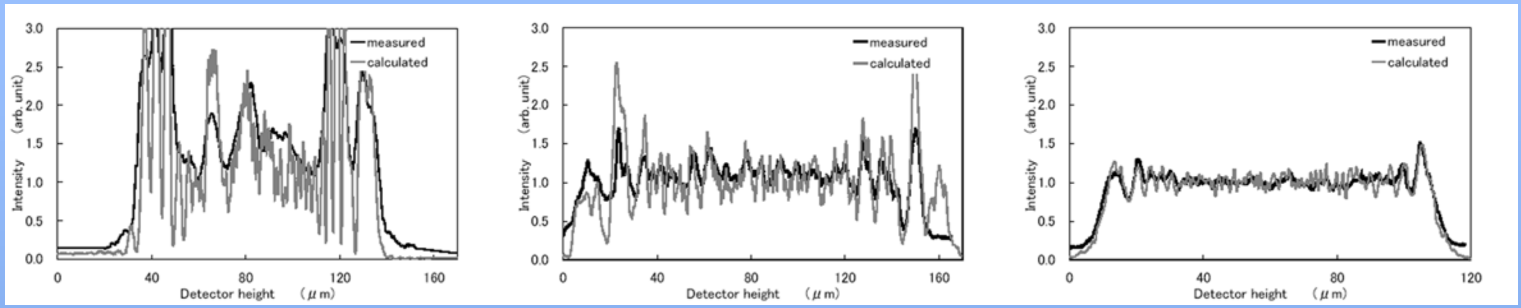

Inverse Problem

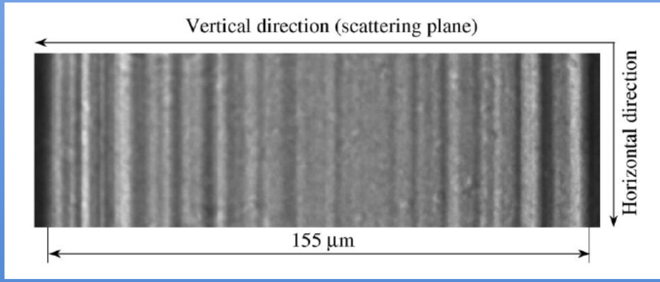

image

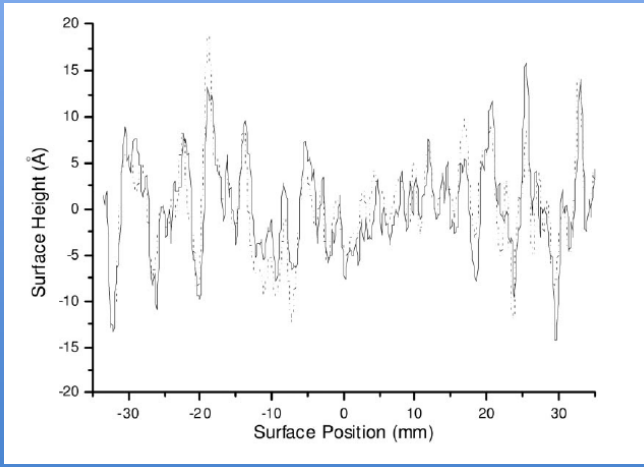

surface
profile

Aspherical Mirror: Nano Focusing

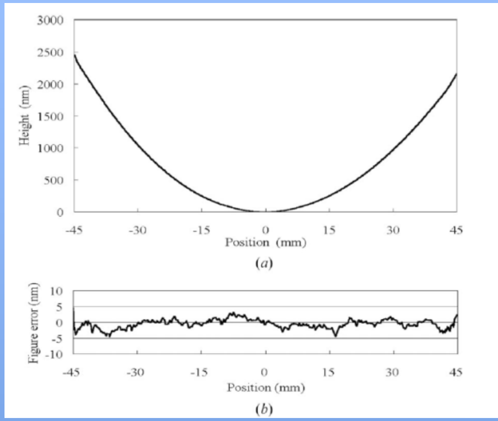

(a) figure and (b) figure error

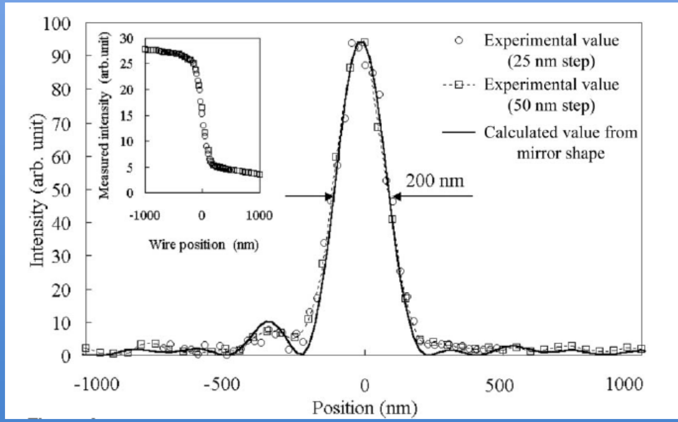

Observed and calculated focal profiles

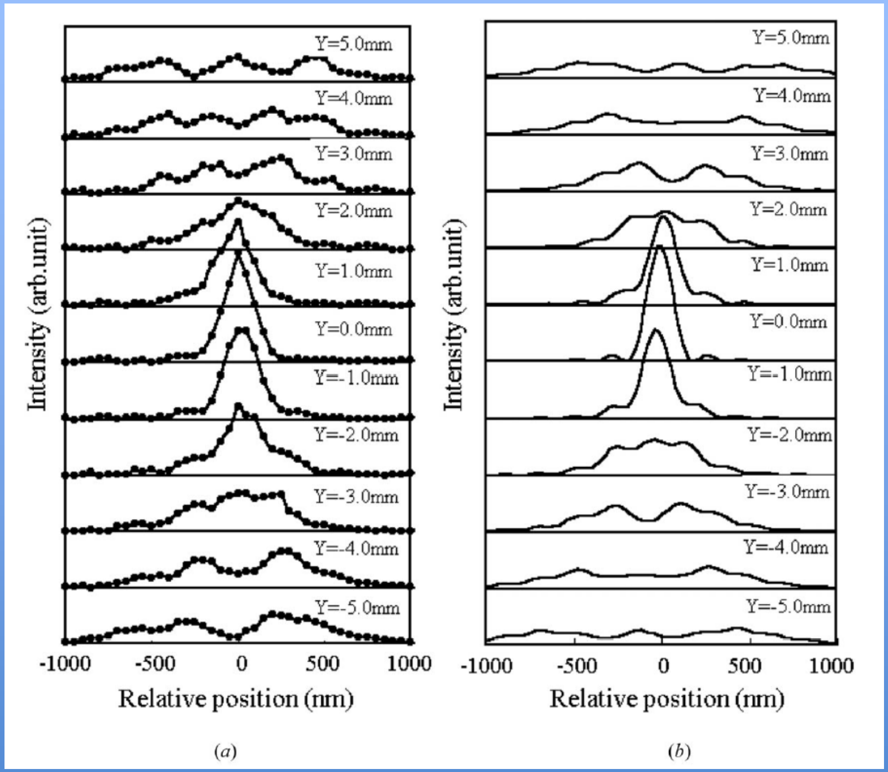

(a) Measured and (b) calculated cross-sectional intensity profiles around the focal spot

Nearly Diffraction-Limited Focusing!

LETTERS
PUBLISHED ONLINE: 22 NOVEMBER 2009 | DOI: 10.1038/NPHYS1457
nature physics

Breaking the 10 nm barrier in hard-X-ray focusing

Hidekazu Mimura[1]*, Soichiro Handa[1], Takashi Kimura[1], Hirokatsu Yumoto[2], Daisuke Yamakawa[1], Hikaru Yokoyama[1], Satoshi Matsuyama[1], Kouji Inagaki[1], Kazuya Yamamura[3], Yasuhisa Sano[1], Kenji Tamasaku[4], Yoshinori Nishino[4], Makina Yabashi[4], Tetsuya Ishikawa[4] and Kazuto Yamauchi[1,3]

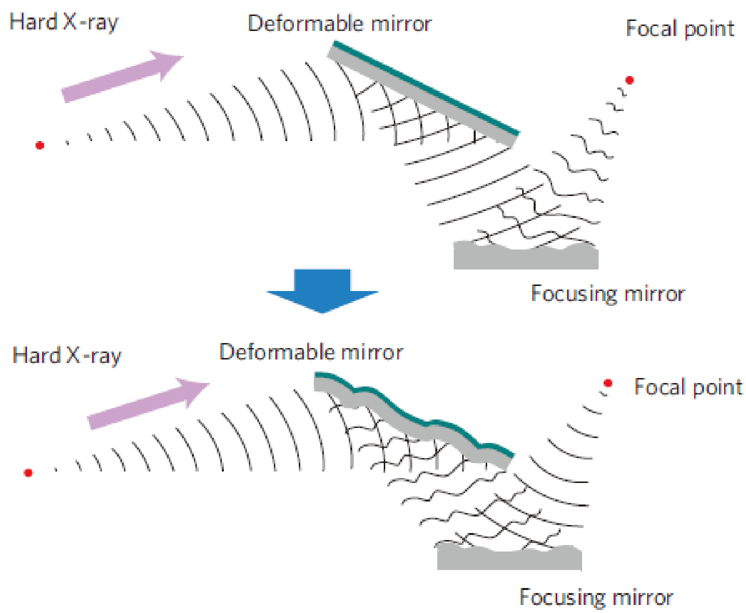

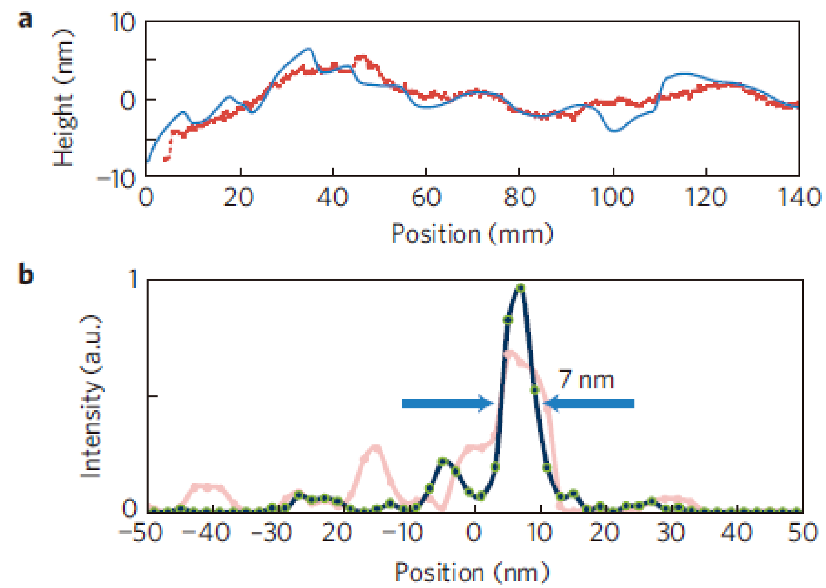

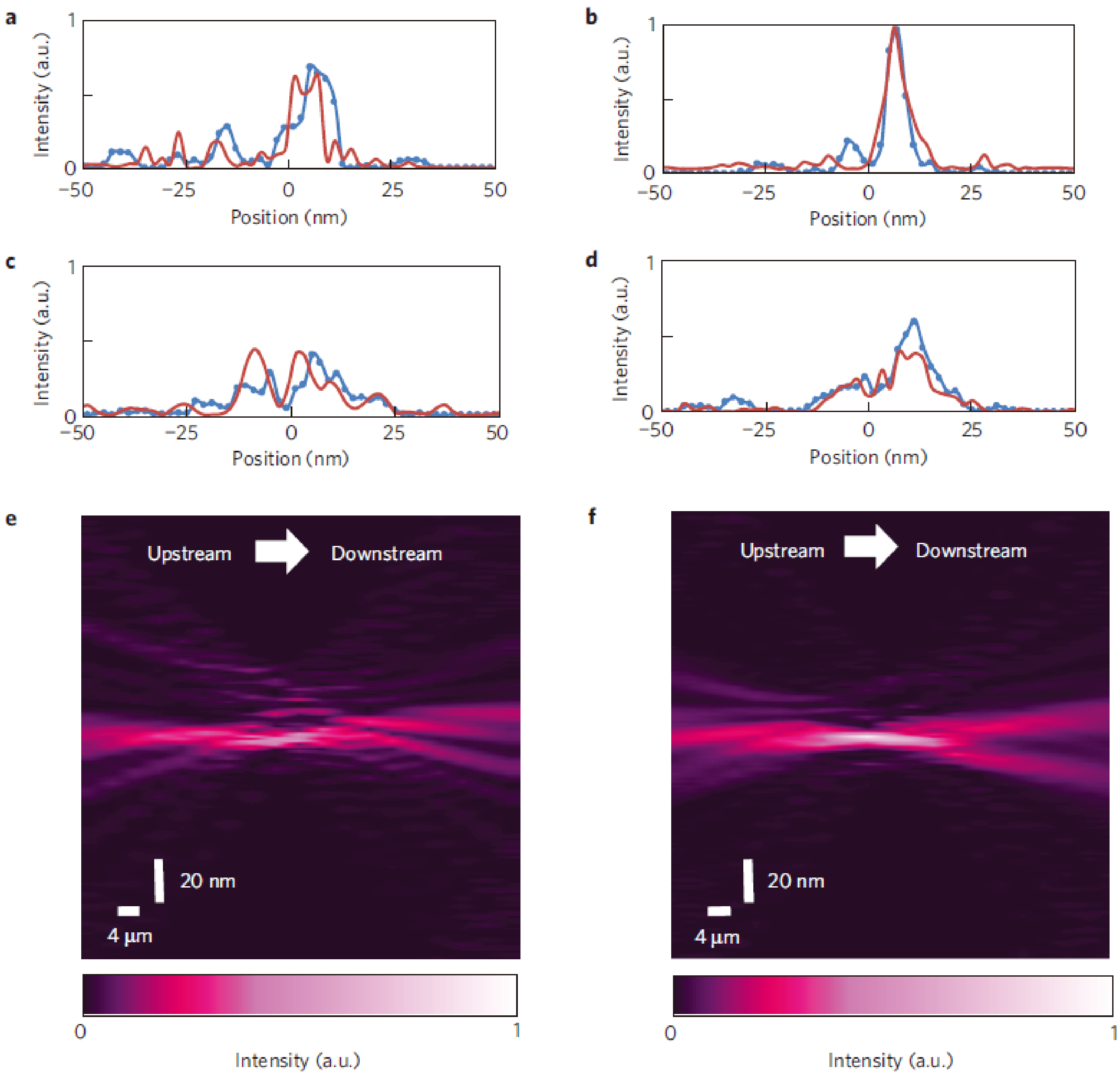

a
b
c
d
Intensity (a.u.)
Position (nm)
1
0
−50
−25
0
25
50
e
f
Upstream
Downstream
20 nm
4 μm
0
1
Intensity (a.u.)

PRL 102, 018101 (2009) PHYSICAL REVIEW LETTERS week ending 9 JANUARY 2009

Three-Dimensional Visualization of a Human Chromosome Using Coherent X-Ray Diffraction

Yoshinori Nishino,[1,*] Yukio Takahashi,[2] Naoko Imamoto,[3] Tetsuya Ishikawa,[1] and Kazuhiro Maeshima[3]
[1]*RIKEN SPring-8 Center, 1-1-1 Kouto, Sayo-cho, Sayo-gun, Hyogo 679-5148, Japan*
[2]*Graduate School of Engineering, Osaka University, 2-1 Yamada-oka, Suita, Osaka 565-0871, Japan*
[3]*Cellular Dynamics Laboratory, RIKEN, 2-1 Hirosawa, Wako, Saitama 351-0198, Japan*
(Received 10 July 2008; revised manuscript received 18 November 2008; published 5 January 2009)

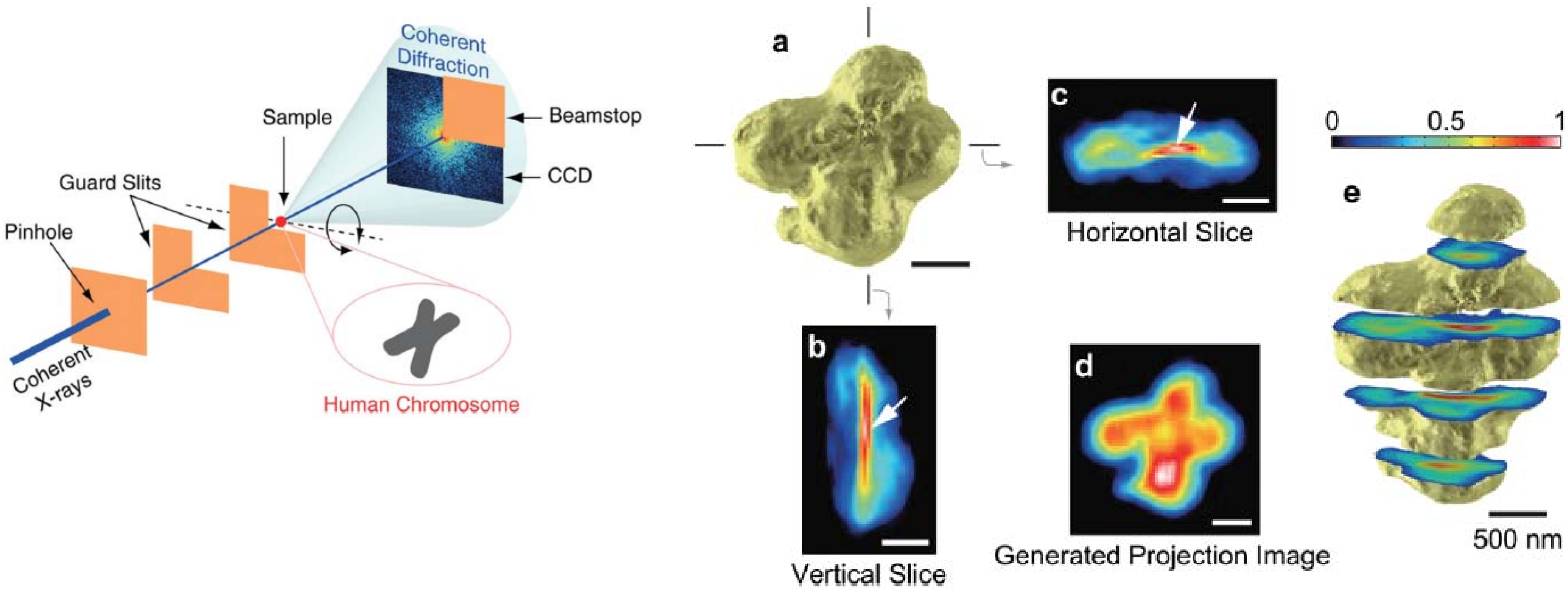

CDI at the BL29XU started in collaboration with John Miao in 2000.
Many 3D observations because of the high beam stability.

NANO LETTERS
pubs.acs.org/NanoLett

Three-Dimensional Electron Density Mapping of Shape-Controlled Nanoparticle by Focused Hard X-ray Diffraction Microscopy

Yukio Takahashi,[*,†] **Nobuyuki Zettsu,**[†] **Yoshinori Nishino,**[§] **Ryosuke Tsutsumi,**[‖] **Eiichiro Matsubara,**[⊥] **Tetsuya Ishikawa,**[#] **and Kazuto Yamauchi**[‡,‖]

[†]Frontier Research Base for Global Young Researchers, Frontier Research Center, Graduate School of Engineering, Osaka University, 2-1 Yamada-oka, Suita, Osaka 565-0871, Japan, [‡]Research Center for Ultra-precision Science and Technology, Graduate School of Engineering, Osaka University, 2-1 Yamada-oka, Suita, Osaka 565-0871, Japan, [§]Research Institute for Electronic Science, Hokkaido University, Sapporo 001-0021, Japan, [‖]Department of Precision Science and Technology, Graduate School of Engineering, Osaka University, 2-1 Yamada-oka, Suita, Osaka 565-0871, Japan, [⊥]Department of Materials Science and Engineering, Kyoto University, Yoshida, Sakyo, Kyoto 606-8501, Japan, and [#]RIKEN SPring-8 Center, Kouto, Sayo-cho, Sayo-gun, Hyogo 679-5148, Japan

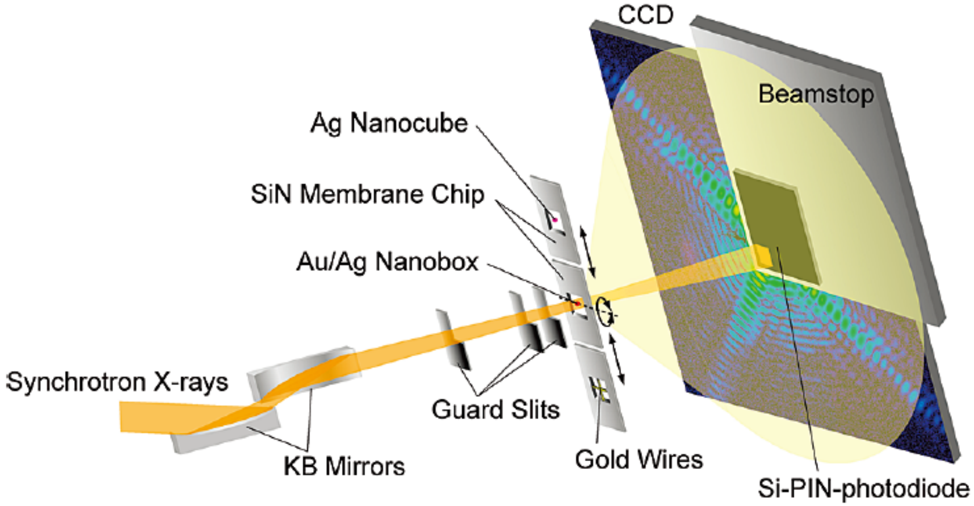

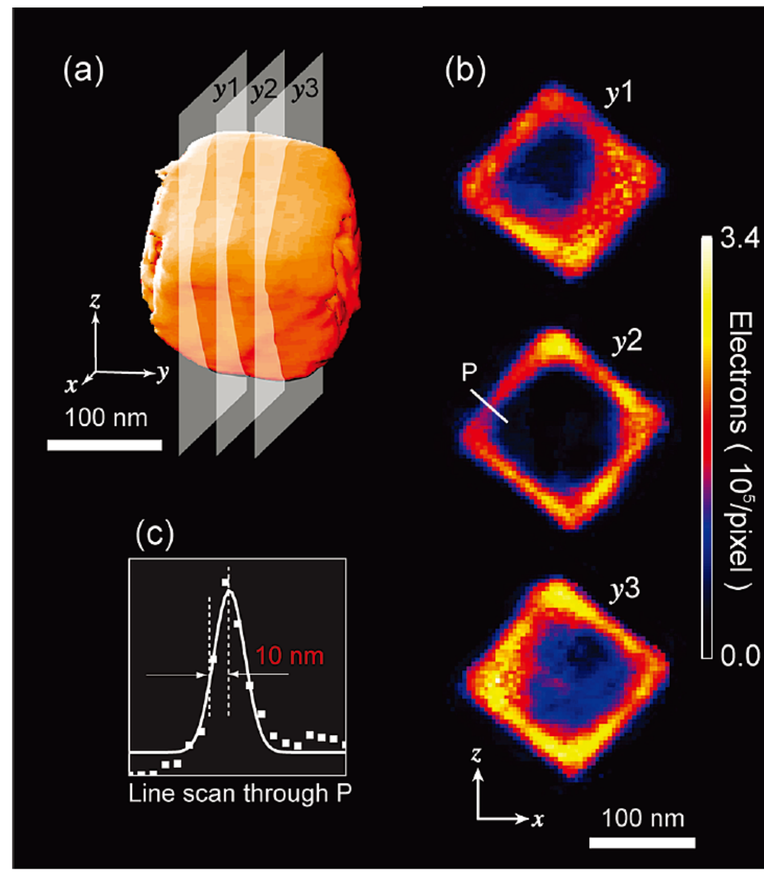

Present Status of Japan X-Ray Free Electron Laser

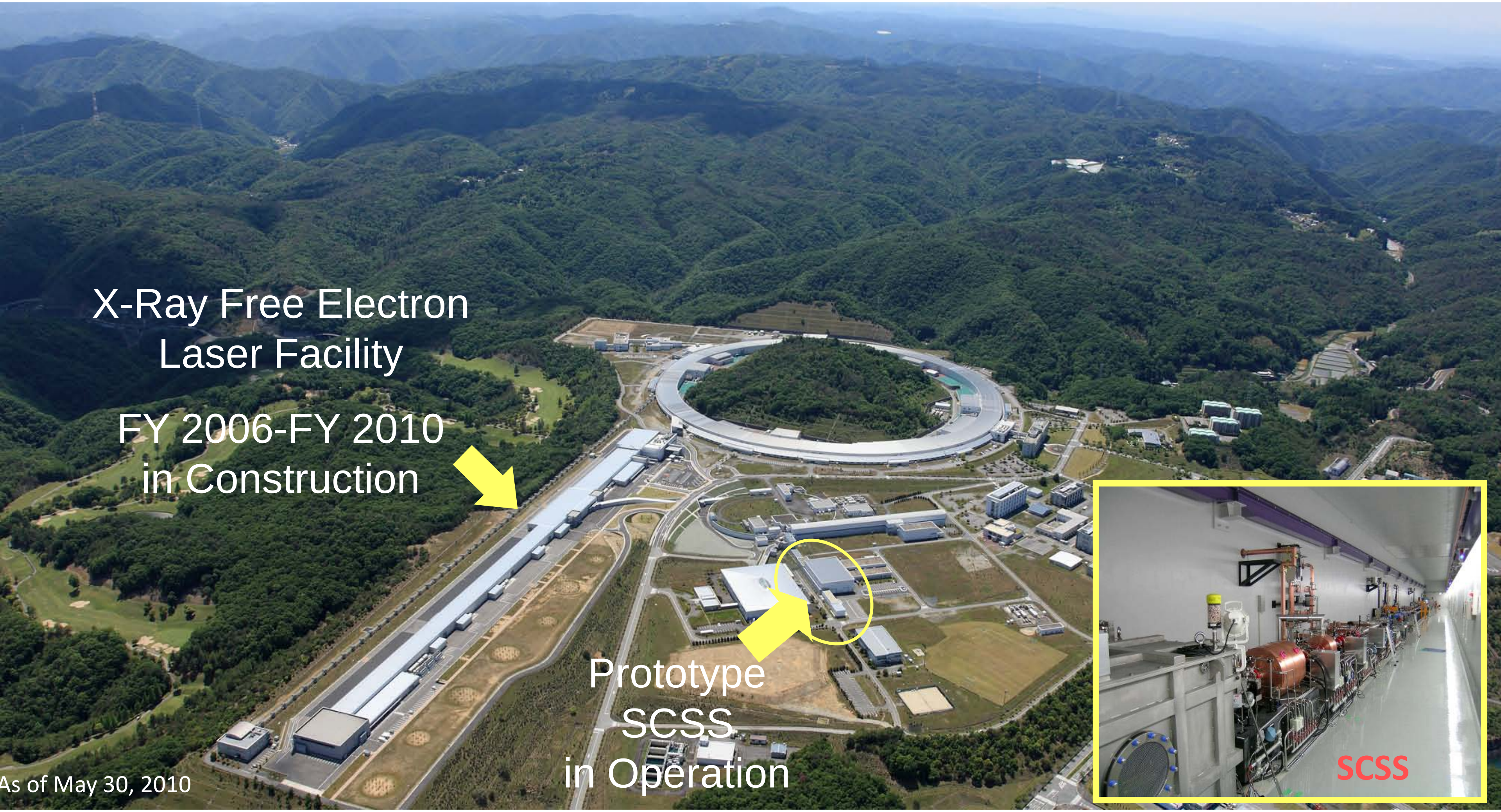

RIKEN
JASRI

SPring-8

Concept

- Compact SASE source with lower energy linac with similar light source performance to bigger sources
- Co-locate with a 3rd generation SR source to be used synergistically

↓

- Use shorter period in-vacuum undulator to reduce the linac energy to lase at <0.1 nm .
- Use high-gradient accelerator tubes (C-Band) to reduce the linac length.

↓

700 m total length, ~400 M$ construction cost, 5 year period

Road Map

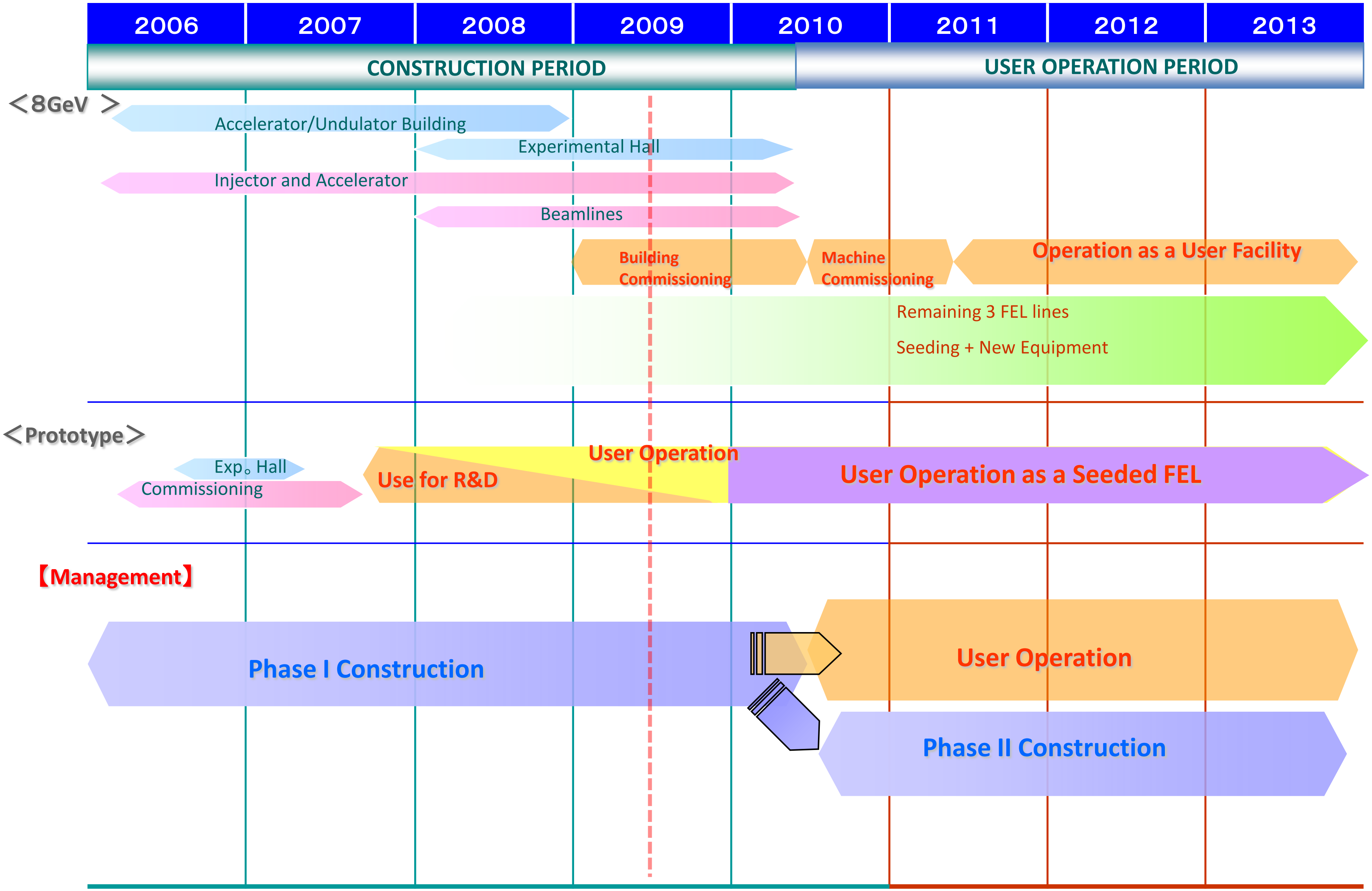

2006
2007
2008
2009
2010
2011
2012
2013
CONSTRUCTION PERIOD
USER OPERATION PERIOD
＜8GeV ＞
Accelerator/Undulator Building
Experimental Hall
Injector and Accelerator
Beamlines
Building Commissioning
Machine Commissioning
Operation as a User Facility
Remaining 3 FEL lines
Seeding + New Equipment
＜Prototype＞
Exp。Hall
Commissioning
Use for R&D
User Operation
User Operation as a Seeded FEL
【Management】
Phase I Construction
User Operation
Phase II Construction

Building Construction

2007/3/23

2008/3/12

2009/3/24

2007/7/27

2008/10/28

2010/5/30

Latest View (1)

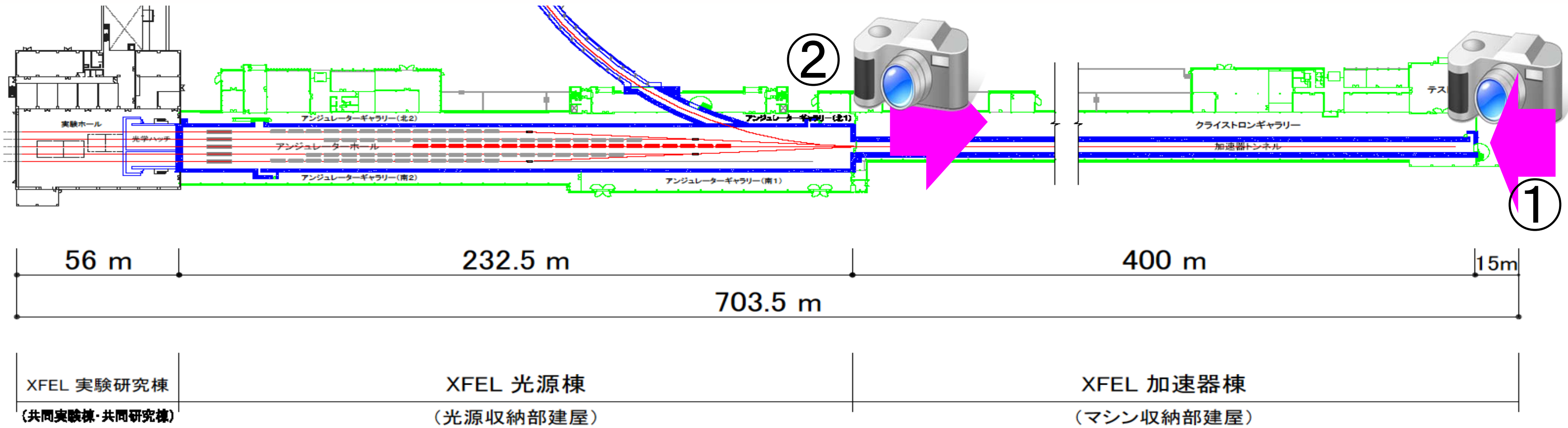

②Klystron Gallery

①Electron Gun & Injector

Latest View (2)

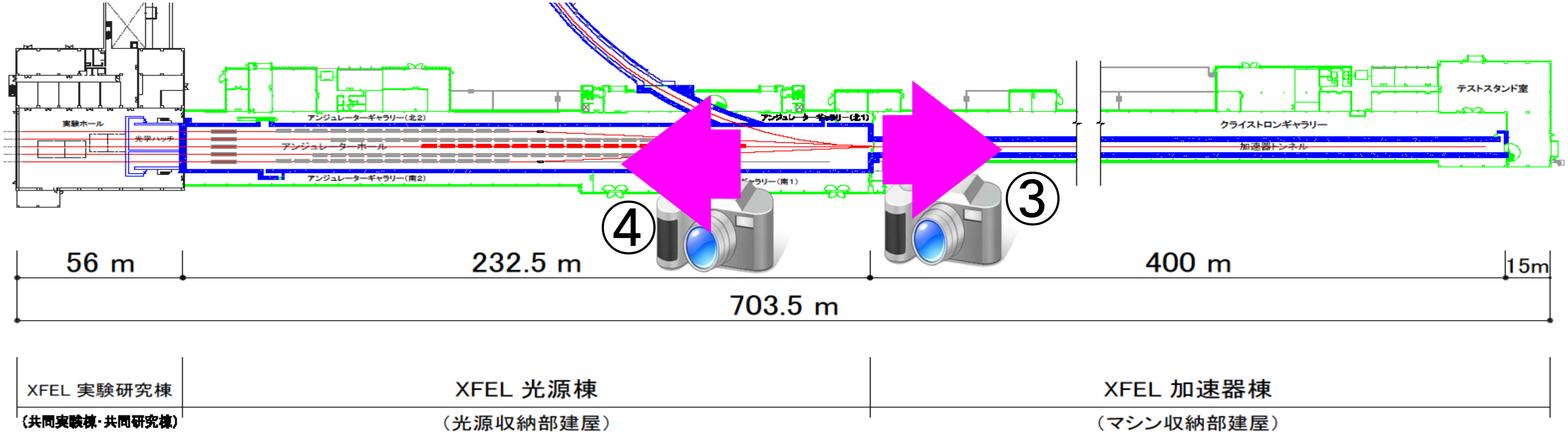

③C-Band Accelerator

④Undulator Gallery

8 GeV X-Ray Free Electron Laser Facility at SPring-8
Total Facility Length ~ 0.7 km

Unique Features

XFEL and SR X-ray beams on the same sample

Short & Low emittance e-beam injection to SP8 from XFEL Linac

Synergistic Use of Two RIKEN-Hosted Key Technologies of National Importance

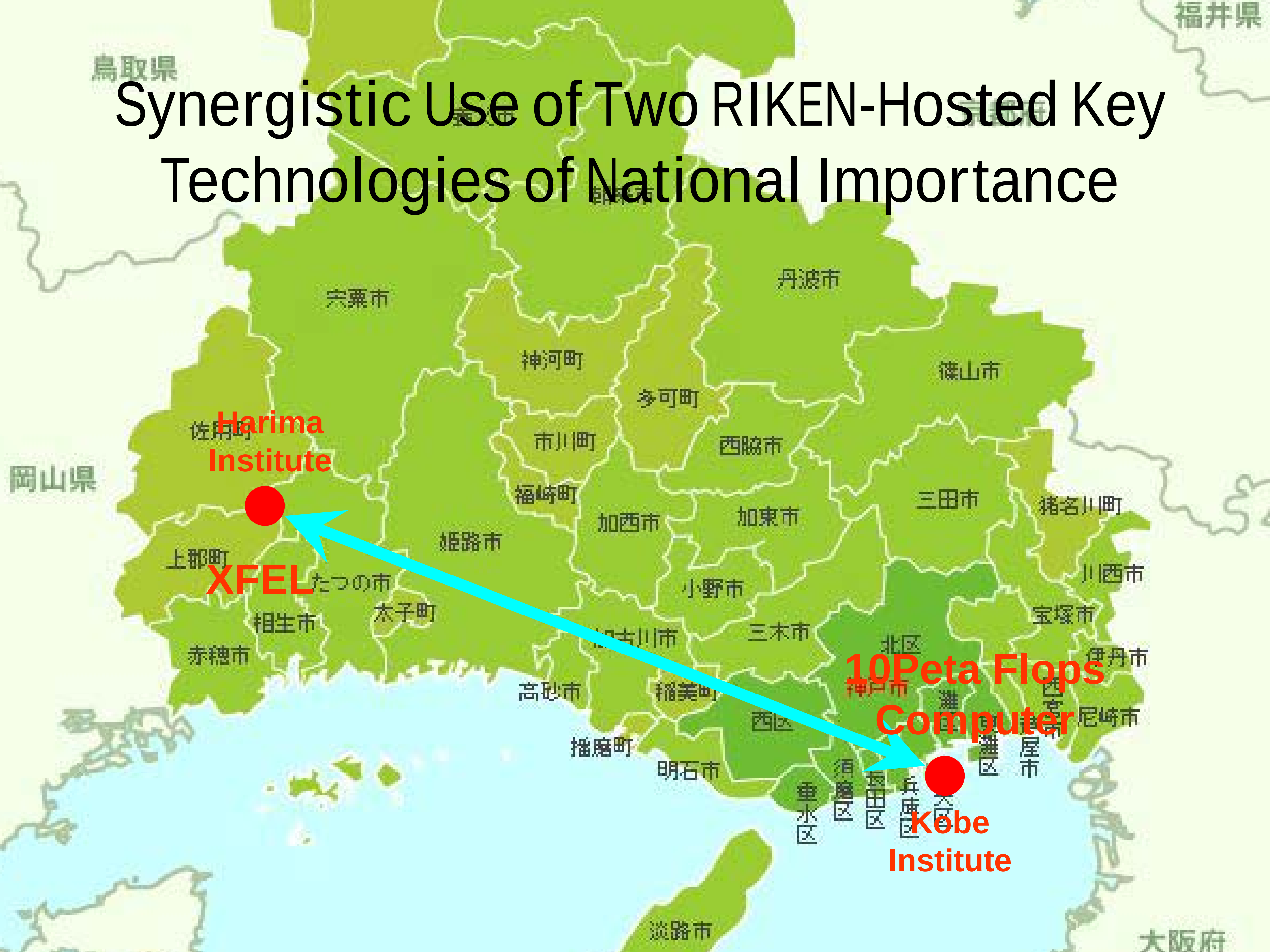

Summary

- X-ray coherence is one of the significant features of the 3rd generation SR sources, and will be similar in the coming SASE-XFEL sources.
- Some applications of coherent x-rays at SPring-8 were shown: Intensity interferometry, Mirror development for nm focusing, and others.
- Present status of the Japan X-Ray Free Electron Laser Project was introduced.
- We believe XFEL is another great example that a new light creates new science and technologies.